Stochastic Model of Neuronal Outgrowth Movement: UNC-5 (UNC5) Regulates the Length and Number of Neuronal Processes in *Caenorhabditis elegans*

Gerard Limerick[*, †], Xia Tang[*, †], Won Suk Lee[*, †], Ahmed Mohamed[*], Aseel Al-Aamiri[*], and William G. Wadsworth[*]

[*]Department of Pathology and Laboratory Medicine, Rutgers Robert Wood Johnson Medical School, Piscataway, NJ 08854

†These authors contributed equally to this work

11 running title: neuronal outgrowth patterning

12

13 key words: neuronal development, axon guidance, asymmetric localization, *Caenorhabditis*

14 *elegans*, netrin and wnt signaling

15

16 corresponding author:

17 William G. Wadsworth

18 Department of Pathology and Laboratory Medicine

19 Rutgers Robert Wood Johnson Medical School

20 675 Hoes Lane West

21 Piscataway, NJ 08854-5635

22 732-235-5768

23 william.wadsworth@rwjms.rutgers.edu

Abstract

Neurons extend processes that vary in number, length, and direction of outgrowth. Extracellular cues help determine the patterning of outgrowth. In *Caenorhabditis elegans,* neurons respond to the extracellular UNC-6 (netrin) cue via UNC-40 (DCC) and UNC-5 (UNC5) receptors. We have postulated that UNC-40 undergoes stochastically orientated asymmetric localization (SOAL) within neurons. Extracellular cues govern the probability of UNC-40 localizing and mediating outgrowth at points along the surface of the neuron. For each instance of time there is a probability that UNC-40-mediated outgrowth will occur in a specific direction and so over time the direction of outgrowth fluctuates. Random walk modeling predicts that the degree of fluctuation affects the extent of outgrowth movement. Therefore, different patterns of outgrowth could be caused by regulating UNC-40 SOAL. Here we present evidence that UNC-5 (UNC5) receptor activity regulates UNC-40 SOAL and affects the length and number of processes that neurons develop. We find that loss of UNC-5 function increases the probability of UNC-40-mediated outgrowth in different directions, thereby increasing the degree of fluctuation. Consistent with the model, in *unc-5* loss-of-function mutants neurons fail to extend processes to full length or fail to develop multiple processes. We further show genetic interactions that suggest the UNC-5 and SAX-3 (Robo) receptors, and the cytoplasmic proteins, UNC-53 (NAV2), MIG-15 (NIK kinase), and MADD-2 (TRIM), function through specific signaling pathways to regulate UNC-40 SOAL in response to the UNC-6 and EGL-20 (wnt) extracellular cues. We propose genes influence the patterning of neuronal outgrowth by regulating the SOAL process.

Introduction

During development, an intricate network of neuronal connections is established. As processes extend from the neuronal cell bodies, distinct patterns of outgrowth emerge. Some extensions remain as a single process, whereas others branch and form multiple processes. If they branch, the extensions can travel in the same or in different directions. Processes vary in length. Extracellular cues are known to influence this patterning, but the underlying logic that governs the formation of patterns remains a mystery.

The secreted extracellular UNC-6 (netrin) molecule and its receptors, UNC-5 (UNC5) and UNC-40 (DCC) are highly conserved in invertebrates and vertebrates, and are known to play key roles in cell and axon migrations. In *Caenorhabditis elegans*, UNC-6 is produced by ventral cells in the midbody and by glia cells at the nerve ring in the head (WADSWORTH *et al.* 1996; WADSWORTH AND HEDGECOCK 1996; ASAKURA *et al.* 2007). It's been observed that neurons that express the receptor UNC-40 (DCC) extend axons ventrally, towards the UNC-6 sources; whereas neurons that express the receptor UNC-5 (UNC5) alone or in combination with UNC-40 extend axons dorsally, away from the UNC-6 sources (HEDGECOCK *et al.* 1990; LEUNG-HAGESTEIJN *et al.* 1992; CHAN *et al.* 1996; WADSWORTH *et al.* 1996).

It is commonly proposed that axons are guided by attractive and repulsive mechanisms (Tessier-Lavigne and Goodman 1996). According to this model, extracellular cues act as attractants or repellants to direct neuronal outgrowth towards or away from sources of the cues. UNC-5 (UNC5) has been described as a "repulsive" netrin receptor because it mediates guidance away from netrin sources (Leung-Hagesteijn et al. 1992; Hong et al. 1999; Keleman and Dickson 2001; Moore et al. 2007). The attraction and repulsion model is deterministic. That is, given the same

conditions, the response of the neuron, attractive or repulsive, will always be the same. As such, the neuronal response to a particular cue is thought to be mediated by attractive or repulsive signaling pathways. In genetic studies, a mutation that disrupts movement towards the cue source denotes gene function within an attractive pathway, whereas mutations that disrupt movement away from a source denotes gene function within a repulsive pathway. Furthermore, the model predicts that the responsiveness of a neuron must switch from attractive to repulsive if the axonal growth cone move towards and then away from the source of a cue.

We have proposed an alternative model in which the movement of neuronal outgrowth is established through a stochastic process. This model is based on evidence indicating that the asymmetrical localization of UNC-40 in the neuron is self-organizing and that the surface to which UNC-40 localizes and mediates outgrowth is stochastically determined (Figure 1A) (Xu *et al.* 2009; Kulkarni *et al.* 2013). Because of this process, which we name "stochastically orientated asymmetric localization" (SOAL), there is a probability that UNC-40-mediated outgrowth will take place at each point along the surface of the neuron. At any instance of time, extracellular cues govern the probability of UNC-40-mediated outgrowth at each point (Kulkarni *et al.* 2013; Tang and Wadsworth 2014; Yang *et al.* 2014). Outgrowth extension can be envisioned as a series of steps, where at each step extracellular cues control the probability for outgrowth in each direction from the point on the surface. This means that over time, the direction of outgrowth movement fluctuates. Such movement can be mathematically described as a random walk, *i.e*. a succession of randomly directed steps (Figure 1B). Random walk movement is diffusive and one property of diffusive motion is that the mean square displacement grows proportionate to the time traveled. Consequently, the more the direction of movement fluctuates, the shorter the distance of travel is in a given amount of time (Figure

1B). In this paper, we propose that UNC-5 helps regulate this fluctuation and, therefore, the extent of outgrowth movement (Figure 1A). In the neuron, this diffusive motion occurs at the micro-scale as innumerable forces act upon the membrane. An increase in diffusive motion at the micro-scale might be observed at the macro-scale as a decrease in the rate of outgrowth.

In this model, guidance cues promote or inhibit outgrowth but they do not intrinsically cause an attractive or repulsive directional response. This is because the direction of outgrowth is determined by a directional bias that is created over time by the combined effect of extracellular cues. In the example illustrated in Figure 2A, a neuronal protrusion experiences an extracellular guidance cue(s) (orange) that is present in a posterior (right) to anterior (left) increasing concentration gradient. This cue acts together with other cues (purple and blue) that set the probability of outgrowth in the dorsal and ventral directions. As long as the probabilities of dorsal and ventral outgrowth are equal, a bias for anterior movement over time is created. For example, at time 1 (Figure 2A top) the probability of anterior outgrowth is 0.8, whereas the probability of dorsal outgrowth is 0.1 and probability of ventral outgrowth is 0.1. As the protrusion travels in the anterior direction it encounters higher levels of the cue. Even if the cue inhibits outgrowth, an anterior directional bias towards the source of that cue can be maintained. For example, at time 2 (Figure 2B bottom), the probability of anterior outgrowth may have been reduced to 0.4 because of the inhibitory effect of the cue. Assuming that signaling mechanisms within the neuron remain relatively constant as the protrusion transverses this environment, the probabilities of dorsal and ventral outgrowth will increase (the sum of the probabilities must equal one because of SOAL). Therefore, the probability of dorsal outgrowth will be 0.3 and the probability of ventral outgrowth will be 0.3 in this example. While this increases the back and forth fluctuation that occurs perpendicular to the

direction of outgrowth, it does not change the directional bias that occurs over time and movement will still be towards the inhibitory cue.

The model makes predictions about patterns of outgrowth in response to extracellular cues. In this example, the neuron's response to the extracellular cues does not have an effect on the directional bias. However, random walk modeling (shown above each diagram and explained in detail later) predicts that a change in the degree to which the direction of outgrowth movement fluctuates will alter the extent of outgrowth. The pattern of outgrowth can be influenced by how great the fluctuation becomes as outgrowth moves towards a source of a cue. For example, if the fluctuation becomes significant as a protrusion moves towards the source, outgrowth will stall before reaching the source. However, if the fluctuation is not great enough at the source of the cue, outgrowth could continue to move forward. This is because the probability of movement in the opposite, inward, direction is low. For instance, a probability of 0.33 anterior, 0.33 dorsal, and 0.33 ventral outgrowth still creates an anterior directional bias. Therefore, in contrast to the attraction and repulsion model, this model does not predict that movement across a source of a cue requires the neuron to switch its responsiveness to the cue.

In the discussion above, a protrusion moves toward the source of an inhibitory cue. However, a similar prediction can be made for movement towards the source of a cue that promotes outgrowth. Assuming that receptor levels at each surface and signaling mechanisms remain relatively constant as the protrusion transverses this environment, the probabilities of dorsal and ventral outgrowth will increase as more receptors at these surfaces are stimulated due to an increasing concentration of the cue. Correspondingly, the probability of outgrowth at the

141 anterior surface will decrease because of SOAL. As with the case of the inhibitory cue, the
142 result is an increase in the degree to which the direction of outgrowth fluctuates.

143

144 The SOAL model makes predictions about how guidance genes might affect outgrowth
145 patterning. The SOAL process allows the direction of outgrowth activity to fluctuate. In Figure
146 2, the relative degree to which UNC-40-mediated (red) and nonUNC-40-mediated (green)
147 outgrowth activity fluctuates under different circumstances is depicted by the extent to which
148 the colored areas cover the neuron's surface. Extracellular cues can influence the degree to
149 which the direction of outgrowth fluctuates (Figure 2A). Likewise, mutations that disrupt the
150 UNC-40 SOAL process could also change the degree to which the direction of UNC-40-mediated
151 outgrowth fluctuates. By altering the extent of outgrowth movement, these genes could
152 regulate the length of a neuron's extension (Figure 2B). In addition to length, the model
153 predicts that the number of processes may be affected. Since extracellular cues are not
154 uniformly distributed across a neuron's surface, the extent of outgrowth movement could vary
155 along the leading-edge surface of a neuron, leading to multiple outgrowths extending in the
156 same direction. Such phenotypes might not have been associated with guidance genes since
157 most genetic studies have focused on only whether movement is disrupted towards or away
158 from the source of a cue. UNC-5, in particular, has been regarded as the quintessential
159 repulsive guidance receptor and *unc-5* mutations are most often interpreted using this
160 perspective.

161

162 Because we observed that UNC-5 affects UNC-40 SOAL (KULKARNI *et al.* 2013), we hypothesized
163 that *unc-5* might regulate the length and number of neuronal processes. Therefore, we decided
164 to look at neuronal outgrowth patterns in *unc-5* mutants for changes in the length and number

165 of processes. In particular, we focused on outgrowth that was not directed away from UNC-6
166 sources since the SOAL model predicts that these outgrowth patterns are not caused by a
167 repulsion mechanism and that they should occur independently of the direction of outgrowth.
168 We further reasoned that if *unc-5* regulates this type of patterning then UNC-40 SOAL might be
169 regulated by specific genetic pathways. We therefore asked whether genetic interactions
170 between *unc-5* and other guidance genes can affect UNC-40 SOAL.

171

172 In this paper, we present genetic evidence that UNC-5 regulates the length and number of
173 processes that neurons development. We argue that these results can be interpreted using the
174 SOAL model. We also show genetic interactions that suggest the UNC-5 and SAX-3 (Robo)
175 receptors, and the cytoplasmic proteins, UNC-53 (NAV2), MIG-15 (NIK kinase), and MADD-2
176 (TRIM), function through specific signaling pathways to regulate UNC-40 SOAL in response to
177 the UNC-6 and EGL-20 (wnt) extracellular cues. Together these results suggest that the SOAL
178 model is useful for understanding how genes regulate patterns of outgrowth.

179

180 **Materials and Methods**

181 **Strains**

182 Strains were handled at 20 ℃ using standard methods (Brenner, 1974) unless stated
183 otherwise. A Bristol strain N2 was used as wild type. The following alleles were used: **LGI**, *unc-*
184 *40(e1430), unc-40(ur304), zdIs5[mec-4::GFP]*; **LGII**, *unc-53(n152)*; **LGIV,** *unc-5(e152), unc-*
185 *5(e53), unc-5(ev480), unc-5(ev585),egl-20(n585), kyIs262[unc-86::myr-GFP;odr-1::dsRed];* **LGIV,**
186 *madd-2(ky592), madd-2(tr103)*; **LGX**, *mig-15(rh148), unc-6(ev400)*, *sax-3(ky123), sax-3(ky200).*
187 Transgenes maintained as extrachromosomal arrays included: *kyEx1212 [unc-86::unc-40-*
188 *GFP;odr-1::dsRed].*

189

190 **Analysis of axon outgrowth and cell body position**

191 HSN neurons were visualized using expression of the transgene *kyIs262[unc-86::myr-GFP].* The
192 mechanosensory neurons, AVM, ALM, and PLM, were visualized using the expression of the
193 transgene *zdIs5[Pmec-4::GFP]*. Synchronized worms were obtained by allowing eggs to hatch
194 overnight in M9 buffer without food. The larval stage was determined by using differential
195 interference contrast (DIC) microscopy to examine the gonad cell number and the gonad size.
196 Staged larvae were mounted on a 5% agarose pad with 10 mM levamisole buffer. Images were
197 taken using epifluorescent microscopy with a Zeiss 63X water immersion objective.

198

199 The number of processes during early L1 larval stage was scored by counting the number of
200 processes that extended for a distance greater than the length of one cell body. We report
201 instances in which there were no such processes, one process or more than one processes. In
202 the L2 larval stage, a single early process was scored if there was only one major extension
203 from the ventral leading edge. The HSN cell body in L2 stage larvae was scored as dorsal if the

204 cell body had failed to migrate ventrally and was not positioned near the PLM axon. In L4 stage
205 larvae, a multiple ventral processes phenotype was scored if more than one major extension
206 protruded from the ventral side of cell body.
207
208 Extension into the nerve ring was scored as defective if the axon did not extend further than
209 approximately half the width of the nerve ring. Anterior extension was scored as defective if
210 the axon did not extend further anteriorly than the nerve ring. PLM axons are scored as over-
211 extending if they extended further anterior than the position of the ALM cell body.
212

213 **Analysis of the direction of HSN outgrowth**

214 HSN was visualized using the transgene *kyIs262[unc-86::myr-GFP].* L4 stage larvae were
215 mounted on a 5% agarose pad with 10 mM levamisole buffer. An anterior protrusion was
216 scored if the axon extended from the anterior side of the cell body for a distance greater than
217 the length of three cell bodies. A dorsal or posterior protrusion was scored if the axon extended
218 dorsally or posteriorly for a distance greater than two cell body lengths. HSN was considered
219 multipolar if more than one process extended a length greater than one cell body. Images were
220 taken using epifluorescent microscopy with a Zeiss 40X objective.
221

222 **Analysis of the UNC-40::GFP localization in L2 stage animal**

223 For analysis of UNC-40::GFP localization, L2 stage larvae with the transgenic marker
224 *kyEx1212[unc-86::unc-40::GFP; odr-1::dsRed]* were mounted on a 5% agarose pad with 10 mM
225 levamisole buffer. Staging was determined by examining the gonad cell number and the gonad
226 size under differential interference contrast (DIC) microscopy. Images were taken using
227 epifluorescent microscopy with a Zeiss 63X water immersion objective. The UNC-40::GFP

228 localization was determined by measuring the average intensity under lines drawn along the
229 dorsal and ventral edges of each HSN cell body by using ImageJ software. For analysis of the
230 anterior–posterior orientation of UNC-40::GFP, the dorsal segment was geometrically divided
231 into three equal lengths (dorsal anterior, dorsal central and dorsal posterior segments). The
232 line-scan intensity plots of each of these segments were recorded. ANOVA test was used to
233 determine if there is a significant difference between intensities of the three segments. The
234 dorsal distribution was considered uniform if $p \geq 0.05$ and was considered asymmetrical if
235 $p \leq 0.05$. Within an asymmetric population, the highest percent intensity was considered to
236 localize UNC-40::GFP to either anterior, posterior or central domain of the dorsal surface.
237

238 **Computations**

239 A program to simulate a two-dimensional lattice random walk based on the probability of
240 dorsal, ventral, anterior, and posterior outgrowth for a mutant (Table 1) was created using
241 MATLAB. (The directions of the axons from multipolar neurons were not scored. These axons
242 appear to behave in the same manner as the axons from monopolar neurons, but this has not
243 yet been tested.) The probability of dorsal, ventral, anterior, or posterior outgrowth was
244 assigned for the direction of each step of a random walk moving up, down, left or right,
245 respectively. Each variable is considered independent and identically distributed. Simulations
246 of 500 equal size steps (size =1) were plotted for 50 tracks (Figure 1B, 5B and 6B inserts). A
247 Gaussian distribution for the final positions of the tracks was generated using Matlab's random
248 function (Figure 6).

249

250 The mean squared displacement (MSD) is used to provide a quantitative characteristic of the

motion that would be created by the outgrowth activity undergoing the random walk. Using the random walks generated for a mutant the MSD can be calculated:

$$msd(\tau) = < [r(t + \tau) - \mathrm{r}(t)]^2 >$$

Here, r(t) is the position at time t and τ is the lag time between two positions used to calculate the displacement, Δr(τ) = r(t+τ) - r(t). The time-average over t and the ensemble-average over the 50 trajectories were calculated. This yields the MSD as a function of the lag time. A coefficient giving the relative rate of diffusion was derived from a linear fit of the curve. The first two lag time points were not considered, as the paths often approximate a straight line at short intervals.

260 **Results**

261 **UNC-5 regulates the pattern of outgrowth from the HSN neuron**

262 To investigate whether UNC-5 activity can regulate the length or number of processes that a
263 neuron can develop when outgrowth is towards an UNC-6 source, we examined the
264 development of the HSN axon in *unc-5* mutations. The HSN neuron sends a single axon to the
265 ventral nerve cord, which is a source of the UNC-6 cue (WADSWORTH *et al.* 1996; ADLER *et al.*
266 2006; ASAKURA *et al.* 2007). Axon formation is dynamic (ADLER *et al.* 2006). Shortly after
267 hatching, HSN extends short neurites in different directions. These neurites, which dynamically
268 extend and retract filopodia, become restricted to the ventral side of the neuron where a
269 leading edge forms. Multiple neurites extend from this surface until one develops into a single
270 axon extending to the ventral nerve cord. Measurements of growth cone size, maximal length,
271 and duration of growth cone filopodia indicate that UNC-6, UNC-40, and UNC-5 control the
272 dynamics of protrusion (NORRIS AND LUNDQUIST 2011).

273

274 We observe that in *unc-5* mutants, the patterns of extension are altered. In wild-type animals at the
275 L1 stage of development most HSN neurons extends more than one short neurite, however in *unc-*
276 *5(e53)* mutants nearly half the neurons do not extend a process (Figures 3A and 3B). During the L2
277 stage in wild-type animals a prominent ventral leading edge forms and the cell body undergoes a
278 short ventral migration that is completed by the L3 stage. By comparison, in *unc-5* mutants the cell
279 body may fail to migrate and instead a single large ventral process may form early during the L2
280 stage (Figures 3A, 3C and 3E). It may be that the ventral migration of the HSN cell body requires the
281 development of a large leading edge with multiple extensions. Together the observations indicate
282 that loss of *unc-5* function affects the patterning of outgrowth, *i.e.* the timing, length, and number of
283 extensions that form. Loss of *unc-5* function does not prevent movement, in fact, a single large

284 ventral extension can form in the mutant at a time that is even earlier than when a single ventral
285 extension can be observed in wildtype.

286

287 We tested four different *unc-5* alleles in these experiments. The *unc-5(e53)* allele is a putative
288 molecular null allele, *unc-5(ev480)* is predicted to truncate UNC-5 after the cytoplasmic ZU-5
289 domain and before the Death Domain, *unc-5(e152)* is predicted to truncate UNC-5 before the
290 ZU-5 domain and Death Domain, and *unc-5(ev585)* is a missense allele that affects a predicted
291 disulfide bond in the extracellular Ig(C) domain (KILLEEN *et al.* 2002). Although both the *unc-*
292 *5(ev480)* and *unc-5(e152)* are predicted to cause premature termination of protein translation
293 in the cytodomain, the *unc-5(e152)* product retains the signaling activity that prevents these
294 phenotypes. Based on other phenotypes, previous studies reported that the *unc-5(e152)* allele
295 retains UNC-40-dependent signaling functions (MERZ *et al.* 2001; KILLEEN *et al.* 2002).

296

297 **UNC-5 is required for the induction of multiple HSN axons by UNC-6ΔC and a *mig-15***
298 **mutation**

299 The results above suggest that UNC-5 activity can regulate the number of HSN extensions that
300 form. To further test this hypothesis, we checked whether loss of UNC-5 function can suppress
301 the development of additional processes that can be induced. Previously we reported that
302 expression of the N-terminal fragment of UNC-6, UNC-6ΔC, induces excessive branching of
303 ventral nerve cord motor neurons and that UNC-5 can suppress this branching (LIM *et al.* 1999).
304 We now report that HSN develops an extra process in response to UNC-6ΔC and that UNC-5
305 suppresses the development of this extra process (Figures 3D and 3F).

306

307 To investigate whether this UNC-5 activity might involve known effectors of asymmetric neuronal
308 outgrowth, we tested for genetic interactions between *unc-5* and both *mig-10* and *mig-15*. MIG-10
309 (lamellipodin) is a cytoplasmic adaptor protein that can act cell-autonomously to promote UNC-40-
310 mediated asymmetric outgrowth (ADLER *et al.* 2006; CHANG *et al.* 2006; QUINN *et al.* 2006; QUINN
311 *et al.* 2008; MCSHEA *et al.* 2013). MIG-15 (NIK kinase) is a cytoplasmic protein and evidence
312 indicates that *mig-15* functions cell-autonomously to mediate a response to UNC-6 (POINAT *et al.*
313 2002; TEULIÈRE *et al.* 2011). It's proposed that *mig-15* acts with *unc-5* to polarize the growth cone's
314 response and that it controls the asymmetric localization of MIG-10 and UNC-40 (TEULIÈRE *et al.*
315 2011; YANG *et al.* 2014). We previously noted that HSN neurons often become bipolar in *mig-15*
316 mutants and frequently UNC-40::GFP is localized to multiple surfaces in a single neuron, suggesting
317 that loss of MIG-15 enhances the ability of UNC-40::GFP to cluster (YANG *et al.* 2014). In our
318 experiments we used the *mig-10 (ct141)* loss-of-function allele (MANSER AND WOOD 1990; MANSER
319 *et al.* 1997) and the *mig-15(rh148)* allele, which causes a missense mutation in the ATP-binding
320 pocket of the kinase domain and is a weak allele of *mig-15* (SHAKIR *et al.* 2006; CHAPMAN *et al.*
321 2008).

322

323 We find that the extra processes induced by UNC-6ΔC expression are suppressed by *mig-*
324 *10(ct141)* (Figures 3F). We also find that the *mig-15* mutation causes extra HSN processes and
325 that the loss of UNC-5 function suppresses these extra HSN processes (Figures 3F and 3G).
326 These results support the hypothesis that the ability of UNC-5 to regulate the development of
327 multiple protrusions involves the molecular machinery that controls UNC-40-mediated
328 asymmetric neuronal outgrowth.

329

330 **UNC-5 is required for PLM overextension**

331 The SOAL model predicts that the ability of UNC-5 to regulate the length and number of neural
332 protrusions is independent of the direction of outgrowth. HSN sends a single axon ventrally, while
333 PLM sends an axon anteriorly from a posteriorly positioned cell body. The HSN axon travels
334 towards UNC-6 sources, whereas the PLM axon pathway is perpendicular to UNC-6 sources. To
335 investigate whether UNC-5 activity can regulate the length or number of processes that develop
336 perpendicular to UNC-6 sources we examined the development of the PLM axon. We also chose
337 PLM because UNC-5 is already known to affect the length of the PLM axon. It was previously
338 reported that in *rpm-1* mutants the PLM axon will overextend in the anterior direction and that
339 this phenotype can be suppressed by *sax-3* and *unc-5* loss-of-function mutations (LI *et al.* 2008).
340 In *rpm-1* loss-of-function mutations there is an increase in the level of UNC-5::GFP expression,
341 suggesting that the level of UNC-5 within PLM is important for controlling overextension.
342 However, the overextension in the *rpm-1* mutant is not suppressed by a loss-of-function *unc-40*
343 mutation (LI *et al.* 2008), suggesting that the overextension does not involve UNC-40 SOAL, but
344 rather another outgrowth activity that is nonUNC-40-mediated.

345

346 Given that UNC-5 activity is involved in the overextension of the PLM axon, and that the *mig-15*
347 mutation affects HSN outgrowth in an UNC-40 dependent fashion, we decided to test whether
348 PLM overextension might be induced by the *mig-15* mutation in an UNC-40-dependent fashion.
349 The HSN results suggest that altering *mig-15* function creates a sensitized genetic background.
350 That is, the *unc-5(ev480)* mutation suppresses HSN outgrowth extension in both the wild-type
351 and *mig-15(rh148)* backgrounds, but the *mig-15* mutation creates a stronger patterning
352 phenotype. This idea is supported by the evidence that the *mig-15* mutation enhances the
353 ability of UNC-40 to localize at surfaces (YANG *et al.* 2014).

354

355 We find that in *mig-15(rh148)* mutants the PLM axon often fails to terminate at its normal
356 position and instead extends beyond the ALM cell body. This overextension is suppressed in
357 *unc-5(e53);mig-15(rh148)* and *unc-40(e1430);mig-15(rh148)* mutants (Figures 4A and 4B).
358 The results are consistent with the idea that UNC-5 is required for the UNC-40-mediated
359 outgrowth activitythat causes overextension in *mig-15(rh148)* mutants.

360

361 **UNC-5 is required for ALM and AVM branching and extension**

362 We also investigated the effect of UNC-5 activity on patterning where sources of UNC-6 and
363 other cues are in a more complex arrangement. Specifically, we examined whether UNC-5 plays
364 a role in the outgrowth of AVM and ALM processes at the nerve ring. During larval
365 development, processes from the AVM neuron and the two ALM neurons (one on each side of
366 the animal) migrate anteriorly to the nerve ring at dorsal and ventral positions respectively
367 (Figure 4C). At the nerve ring each axon branches; one branch extends further anteriorly and the
368 other extends into the nerve ring. Evidence suggests that at the midbody of the animal the
369 positioning of these axons along the dorsal-ventral axis requires UNC-6, UNC-40, and UNC-5
370 activity. In *unc-6*, *unc-40,* and *unc-5* null mutants, or when the UNC-6 expression pattern is altered,
371 the longitudinal nerves are mispositioned (REN *et al.* 1999). Glia cells and neurons at the nerve ring
372 are sources of UNC-6 (WADSWORTH *et al.* 1996). The guidance of some axons in the nerve ring are
373 disrupted in *unc-6* and *unc-40* mutants (HAO *et al.* 2001; YOSHIMURA *et al.* 2008). The precise
374 spatial and temporal arrangement of the UNC-6 cue in relationship to the position of the
375 migrating growth cones is not fully understood. Nevertheless, the anteriorly migrating growth
376 cones appear to use the UNC-6 cue from the ventral sources to help maintain the correct dorsal-
377 ventral position, even while moving towards the nerve ring, which is a new source of UNC-6
378 that is perpendicular to the ventral source. At the nerve ring the axons branch. One process

379 continues anteriorly, moving past the new UNC-6 source, whereas the other projects at a right
380 angle and moves parallel to the new source.

381

382 We find genetic interactions involving *unc-5, unc-40,* and *mig-15* that affect outgrowth
383 patterning of the ALM and AVM extensions at the nerve ring (Figures 4C, 4D, and 4E). In *mig-*
384 *15(rh148);unc-5(e53)* mutants, the AVM axon often fails to extend anteriorly from the branch
385 point and only extends into the nerve ring, or it fails to extend into the nerve ring and only
386 extends anteriorly, or it fails to do both and terminates at this point. In *unc-40(e1430)* mutants,
387 the axon often fails to branch into the nerve ring, although it extends anteriorly. In comparison,
388 in *unc-40(e1430);mig-15(rh148)* mutants more axons extend into the nerve ring. These results
389 suggest that UNC-5 helps regulate UNC-40-mediated outgrowth to pattern the outgrowth at the
390 nerve ring.

391

392 **Interactions between *unc-5* and other genes affect the probability of HSN extension in**
393 **each direction**

394 We hypothesize that there are interactions between *unc-5* and other genes that control the
395 degree to which the direction of outgrowth fluctuates. In the SOAL model, the collective effect
396 of all the cues that promote and inhibit outgrowth set a probability of outgrowth at each
397 surface at each instance of time. As the direction of outgrowth fluctuates over time, a bias is
398 created that determines directionality. Since the direction of outgrowth is stochastically
399 determined, gene activity is not inherently associated with movement in a specific direction.
400 This model differs from the attraction and repulsion model where gene activity is assayed
401 based on direction, *i.e.* the direction of movement relative to the source of a cue. The attraction
402 and repulsion model places genes into attractive or repulsive pathways. We hypothesize that

403 *unc-5* and other genes might instead be ordered into pathways based on how they affect the
404 fluctuation of outgrowth activity.

405

406 Probability distributions for the direction of outgrowth are used to study how genes affect the
407 fluctuation of outgrowth activity. By comparing the distributions created from wild-type and
408 mutant animals, the relative effect that genes have on the fluctuation can be determined. To
409 accomplish this, the direction that the HSN axon initially projects from the cell body is scored
410 (Figure 5A). We reason that the initial development of an axon is the result of the collective
411 impact of all the individual outgrowth movements that take place during the initial formation of
412 the axon. In wildtype, there is a high probability for outgrowth in the ventral direction at each
413 instance of time. As such, there is little fluctuation over time and a strong bias for ventrally
414 directed outgrowth is created. A mutation can cause a lower probability of outgrowth in the
415 ventral direction and a higher probability for outgrowth in other directions. This creates
416 greater fluctuation over time and a weaker bias of ventrally directed outgrowth. For this assay,
417 all the outgrowth movement during the initial axon extension is treated as a single event, *i.e.* the
418 movement of the membrane occurs in a single step from the cell body to a position that is at a
419 set length from the cell body (see Materials and Methods). This step is in the anterior,
420 posterior, dorsal, or ventral direction. Thus, direction is the random variable which takes a
421 value of anterior, posterior, dorsal, or ventral. We can determine the probability of occurrence
422 for each value by scoring many individual animals for each strain.

423

424 Using this assay, we tested for genetic interactions between *unc-5* and four other genes; *elg-20,*
425 *sax-3, madd-2,* or *unc-6.* We have chosen these particular genes because previous observations
426 suggest interactions. 1) EGL-20 (Wnt) is a secreted cue expressed from posterior sources (PAN

427 *et al.* 2006) and it affects to which surface of the HSN neuron the UNC-40 receptor localizes and
428 mediates outgrowth (KULKARNI *et al.* 2013). Based on a directional phenotype, a synergistic
429 interaction between *unc-5* and *egl-20* has been observed. In either *unc-5* or *egl-20* mutants the
430 ventral extension of AVM and PVM axons is only slightly impaired, whereas in the double
431 mutants there is much greater penetrance (LEVY-STRUMPF AND CULOTTI 2014). 2) SAX-3(Robo) is
432 a receptor that regulates axon guidance and is required for the asymmetric localization of UNC-
433 40 in HSN (TANG AND WADSWORTH 2014). Based on a directional phenotype, SAX-3 and UNC-40
434 appear to act in parallel to guide the HSN towards the ventral nerve cord (XU *et al.* 2015). 3)
435 MADD-2 is a cytoplasmic protein of the tripartite motif (TRIM) family that potentiates UNC-40
436 activity in response to UNC-6 (ALEXANDER *et al.* 2009; ALEXANDER *et al.* 2010; HAO *et al.* 2010;
437 MORIKAWA *et al.* 2011; SONG *et al.* 2011; WANG *et al.* 2014). MADD-2::GFP and F-actin colocalize
438 with UNC-40::GFP clusters in the anchor cell (WANG *et al.* 2014). 4) Of course, UNC-6 is an UNC-
439 5 ligand. DCC (UNC-40) and UNC5 (UNC-5) are thought to act independently or in a complex to
440 mediate responses to netrin (UNC-6) (COLAVITA AND CULOTTI 1998; HONG *et al.* 1999; MACNEIL *et*
441 *al.* 2009; LAI WING SUN *et al.* 2011).

442

443 In a test for interaction with *egl-20*, we find that in comparison to *unc-5(e53)* or *egl-20(n585)*
444 mutants, the *unc-5(e53);egl-20(n585)* double mutant have a lower probability for ventral
445 outgrowth and higher probability for outgrowth in other directions (Table 1). This suggests
446 that *unc-5* and *egl-20* may act in parallel to achieve the highest probability for HSN ventral
447 outgrowth, *i.e.* they act to prevent UNC-40-mediated outgrowth from fluctuating in other
448 directions.

449

450 In a test for interaction with *sax-3,* we find that the probability of outgrowth in each direction in
451 *unc-5(e53);sax-3(ky200)* mutants is similar to the probabilities in *sax-3(ky200)*or *sax-3(ky123)*
452 mutants (Table 1). Given the results with *unc-5* and *egl-20*, we further tested the probability of
453 outgrowth in each direction in *egl-20(n585);sax-3(ky123)* mutants. We find that it is similar to
454 the probabilities in *sax-3(ky200)*or *sax-3(ky123)* mutants (Table 1). The *sax-3(ky123)* allele
455 results in a deletion of the signal sequence and first exon of the gene, whereas sax-3(ky200)
456 contains a missense mutation which is thought to cause protein misfolding and mislocalization
457 at the restrictive temperature (25°C) (ZALLEN *et al.* 1998; WANG *et al.* 2013). The *egl-*
458 *20(n585);sax-3(ky123)* mutants do not grow well and so it is easier to use the temperature sensitive
459 *sax-3* allele. Together, the results suggest that *sax-3* may be required for both the *unc-5-* and the
460 *egl-20*-mediated activities that allow the highest probability for HSN ventral outgrowth.

461

462 In a test for interaction with *madd-2,* we find that the probability of outgrowth in each direction in
463 *unc-5(e53);madd-2(tr103)* mutants is similar to the probabilities in *madd-2(tr103)* mutants (Table 1).
464 There is a higher probability for anterior HSN outgrowth, similar to what is observed in *unc-*
465 *40(e1430)* mutants. These results suggest that *madd-2* might be required for the *unc-40*
466 outgrowth activity. The probability of outgrowth in each direction in *madd-2(tr103);sax-*
467 *3(ky123)* mutants is similar to the probabilities in *sax-3(ky200)*or *sax-3(ky123)* mutants (Table
468 1). The *madd-2(tr103)* allele appears to act as a genetic null (ALEXANDER *et al.* 2010).

469

470 In a test for interaction with *unc-6,* we find that the probability of outgrowth in each direction
471 in *unc-5(e53);unc-6(ev400)* and *unc-40(e1430);unc-5(e53)* mutants is similar to the probabilities
472 in *unc-6(ev400)* mutants insofar as there is a lower probability for ventral outgrowth and a
473 higher probability for anterior outgrowth (Table 1). However, the probabilities in each

474 direction are closer to those obtained from the *unc-40(e1430)* mutants because the probability
475 of anterior outgrowth is lower in these mutants than in *unc-6* mutants. This suggest that UNC-5
476 and UNC-40 might help increase the probability of anterior outgrowth in the absence of UNC-6.

477

478 Taken together, these results support the hypothesis that there are genetic interactions that
479 regulate the degree to which the direction of outgrowth fluctuates. Rather than defining the
480 function of a gene by its ability to control a deterministic event, *i.e.* outgrowth in one direction,
481 gene function can be defined by its ability to control a stochastic process, *i.e.* the probability of
482 outgrowth in different directions.

483

484 ***unc-5* is a member of a class of genes that has a similar effect on the spatial extent of movement**

485 How does *unc-5* affect outgrowth movement? The results above show that *unc-5* and its
486 interactions with other genes affect the degree to which the direction of outgrowth fluctuates.
487 The degree of fluctuation differs depending on the genes involved. The SOAL model predicts
488 that these differences alter the extent of outgrowth; the more the direction of movement
489 fluctuates, the shorter the distance of travel is in a given amount of time.

490

491 To depict how *unc-5* and other genes differentially regulate outgrowth movement, we use
492 random walk modeling. Random walks describe movement that occurs as a series of steps in
493 which the angles and the distances between each step is decided according to some probability
494 distribution. By using the probability distribution obtained from a mutant for each step of a
495 random walk, and by keeping the distance of each step equal, a random walk can be
496 constructed (Figure 5A). In effect, this method applies the probability distribution to discrete

497 particles having idealized random walk movement on a lattice. By plotting random walks
498 derived from wild-type animals and different mutants, the relative effect that mutations have
499 on random walk movement can be visualized. For example, Figure 5B shows 50 tracks of 500
500 steps for wildtype and two mutants (mutant A is *unc-5(e53)* and mutant B is *egl-20(n585);sax-*
501 *3(ky123)*). This reveals the effect that a mutation has on the displacement of movement. After
502 500 steps the displacement from the origin (0,0) is on average less for mutant A than for
503 wildtype, and less for mutant B than for wildtype or mutant A.

504

505 The random walk models show the relative effect that a mutation has on a property of
506 outgrowth movement. It is worth noting that this is not modeling the actual trajectory of
507 migrating axons. Neuronal outgrowth is essentially a mass transport process in which mass
508 (the molecular species of the membrane) is sustained at the leading edge and moves outward.
509 Our assay compares the effect that different mutations would have on the movement of mass at
510 the leading edge of an extension if the conditions of the system were kept constant. Of course,
511 *in vivo* the conditions are not constant. For one, as an extension moves it will encounter new
512 environments where the cues may be new or at different concentrations, all of which affect the
513 probability distribution. The actual patterns of outgrowth observed are the result of all the
514 probabilities for outgrowth that occur at each instance of time. It has recently been suggested
515 that our description might be more accurately described as neuro-percolation, a superposition
516 of random-walks (AIELLO 2016).

517

518 Our random walk analysis compares the effect that different mutations have on the properties
519 of movement. In wild-type animals, there is a high probability for outgrowth in the ventral
520 direction. The analysis shows that conditions in wildtype create nearly straight-line movement,

521 *i.e.* if the same random walk is repeatedly done for the same number of steps, starting at the
522 same origin, the final position of the walk along the x axis does not vary a great amount. In
523 comparison, we find that a mutation can create random walk movement in which the final
524 position is more varied. This variation occurs because the mutation increases the probability of
525 outgrowth in other directions. For each mutation, we simulate 50 random walks of 500 steps
526 and derive the mean and standard deviation of the final position along the X-axis. To compare
527 strains, we plot the normal distribution, setting the mean at the same value for each. The
528 difference between the curve for a mutant and wildtype shows the degree to which the
529 mutation caused the direction of outgrowth to fluctuate (Figure 5C).

530

531 The results reveal four different distribution patterns (Figure 6). The first class is the wild-type
532 distribution, which has the distribution curve with the highest peak. The second class
533 comprises *unc-5, egl-20, unc-53,* and *unc-6* in which the distribution curve is flatter than the
534 wild-type curve. We included *unc-53* because our previous study showed that it has genetic
535 interactions with *unc-5* and *unc-6* (KULKARNI *et al.* 2013). The *unc-53* gene encodes a
536 cytoskeletal regulator related to the mammalian NAV proteins and *unc-53* mutations cause
537 guidance defects (MAES *et al.* 2002; STRINGHAM *et al.* 2002; STRINGHAM AND SCHMIDT 2009). The
538 third class has a distribution curve which is flatter than the second and comprises *sax-3, mig-15,*
539 and several double mutation combinations (Figure 6). The fourth class has the flattest
540 distribution curve and comprises *egl-20;sax-3*, *unc-40;sax-3,* and *unc-53;sax-3;unc-6*. This class
541 indicates the greatest degree of fluctuation. The ability to cause the direction of movement to
542 fluctuate is not associated with a specific direction of HSN movement. For example, *unc-5;sax-3,*
543 *unc-53;unc-6, unc-40;egl-20,* and *madd-2;sax-3* each show a widely dispersed pattern, but the
544 direction is ventral, dorsal, anterior, and posterior, respectively (Figure 6).

545

546 The distribution patterns indicate that genes have different effects on the extent that outgrowth
547 movement can travel through the environment. Mean squared displacement (MSD) is a
548 measure of the spatial extent of random motion. The MSD can be calculated from the random
549 walk data. Plotting MSD as a function of the time interval shows how much an object displaces,
550 on average, in a given interval of time, squared (Figure 7A). For normal molecular diffusion, the
551 slope of the MSD curve is directly related to the diffusion coefficient. In cell migration models
552 this value is referred to as the random motility coefficient. Coefficients are experimentally
553 determined; they describe how long it takes a particular substance to move through a
554 particular medium. We determine this value in order to numerically and graphically compare
555 how mutations can alter displacement relative to wildtype (Figure 7B). The four classes of
556 genes are apparent by comparing the height of the bars in Figure 7B.

557

558 The results of this modeling suggest that the activities of certain genes, and combinations of
559 genes, have distinct effects on the rate of outgrowth movement. In theory, these differences
560 could be an important means by which genes cause different outgrowth patterns.

561

562 ***unc-5* and other genes regulate UNC-40 receptor clustering, which is a consequence of the**
563 **SOAL process**

564 How does *unc-5* affect the localization of the UNC-40 receptor and how does this localization
565 affect UNC-40-mediated outgrowth activity and the pattern of outgrowth? Beginning in the
566 early L2 stage, UNC-40::GFP becomes localized to the ventral side of HSN in wildtype (ADLER *et*
567 *al.* 2006; KULKARNI *et al.* 2013). Reflecting the dynamic morphological changes that occur as the
568 HSN axon forms, the site of asymmetric UNC-40::GFP localization alternates in the neurites and

569 along the ventral surface of the neuron (KULKARNI *et al.* 2013). Dynamic UNC-40::GFP
570 localization patterns have also been reported for the anchor cell, in which UNC-40 and UNC-6
571 are also key regulators of extension (ZIEL *et al.* 2009; HAGEDORN *et al.* 2013). Live imaging of the
572 anchor cell reveals that UNC-40::GFP "clusters" form, disassemble, and reform along the
573 membrane (WANG *et al.* 2014). However, live imaging can't directly ascertain whether the
574 position of a cluster is randomly determined since a movement event cannot be repeatedly
575 observed to determine a probability distribution. Mathematical modeling of cluster movement
576 as a stochastic process has not been done. Nevertheless, the results are consistent with the fact
577 that a probability distribution for the direction of UNC-40-mediated HSN outgrowth movement
578 can be determined and, therefore, the UNC-40 localization that gives rise to the outgrowth
579 activity can be defined as a stochastic process.

580

581 The UNC-40::GFP clustering phenomena raises questions about the relationship between
582 robust UNC-40 clustering (*i.e.,* sites of distinct UNC-40 localization observable by UNC-40::GFP)
583 and UNC-40-mediated outgrowth activity. Two models are presented in Figure 8. In the first
584 model, the SOAL mechanism causes UNC-40 clustering, which is required for UNC-40-mediated
585 outgrowth activity (Figure 8A). In the second model, SOAL and outgrowth activities are
586 independent and can happen concurrently (Figure 8B). In the first model, the output of the
587 SOAL process is receptor clustering. This is next followed by outgrowth activity from the
588 locations at the membrane where the clusters become stable. This model renders UNC-40-
589 mediated outgrowth a deterministic event occurring at the macro-scale. In the second model,
590 the SOAL process and outgrowth activity are concurrent activities which can occur
591 stochastically along the membrane at the micro-scale. UNC-40 clustering in this model might be
592 an observable consequence of the micro-scale stochastic process that arises over time.

593

594 The models make specific predictions that can be tested. In the first model, UNC-40-mediated
595 outgrowth will not happen if UNC-40 does not cluster. In the second model, the loss of UNC-40
596 clustering does not lead to a loss of UNC-40-mediated outgrowth. We favor the second model.
597 In the *sax-3* mutant there is a large fluctuation in the direction of outgrowth; it is in the third
598 class of mutants (Figures 6 and 7). We previously reported that *sax-3* is required for robust
599 UNC-40::GFP asymmetric localization; in *sax-3* mutants UNC-40::GFP remains uniformly
600 dispersed around the periphery of HSN ((TANG AND WADSWORTH 2014) and Figure 9). Whereas
601 in the *sax-3* mutant there is a ventral bias for outgrowth, in the *unc-40;sax-3* mutant there is not
602 (Figure 6). This suggests that in the *sax-3* mutant there is UNC-40-mediated outgrowth activity
603 that helps create a ventral bias. This is consistent with the second model because UNC-40-
604 mediated outgrowth activity is occurring even when robust UNC-40::GFP is not observed.

605

606 We hypothesize that a consequence of the micro-scale SOAL process over time is macro-scale
607 UNC-40 clustering. If so, then *unc-5* activity should affect UNC-40::GFP clustering because it
608 affects the degree to which the direction of UNC-40 receptor localization fluctuates. However,
609 even though there is a higher probability that localization occurs at surfaces other than at the
610 ventral surface, we observe robust asymmetrically localized UNC-40::GFP clustering in *unc-*
611 *5(e53)* mutants (KULKARNI *et al.* 2013). We speculate that *unc-5(e53),* as well as other gene
612 mutations, do not cause the direction of UNC-40 localization to fluctuate enough to prevent
613 observable UNC-40::GFP clustering. We decided to examine UNC-40::GFP clustering in double
614 mutants to see whether there is an additive effect. In double mutants will the direction of UNC-
615 40 localization fluctuate enough so that UNC-40::GFP clustering cannot be observed in our
616 assay?

617

618 We made double mutant combinations between *unc-5*, and *egl-20* or *unc-53.* In *egl-20* and *unc-*
619 *53* single mutants there is fluctuation in the direction of outgrowth (Figures 6 and 7) and
620 robust asymmetrical UNC-40::GFP localization (Figure 9, *unc-53* results were previously
621 reported (KULKARNI *et al.* 2013)). In comparison to the single mutants, the double mutants all
622 show an increase in the degree to which the direction of outgrowth fluctuates (Figures 6 and 7).
623 Further, in contrast to the single mutants, UNC-40::GFP remains uniformly dispersed around
624 the periphery of HSN in the double mutants (Figure 9). The results suggest a correlation
625 between the degree to which UNC-40-mediated outgrowth activity fluctuates and the ability to
626 detect UNC-40::GFP clustering. This is consistent with the second model (Figure 8). We also
627 observe that in *madd-2(tr103)* mutants the direction of outgrowth fluctuates (Table 1), but
628 unlike *egl-20* and *unc-53* single mutants, there is not robust asymmetrical UNC-40::GFP
629 localization and UNC-40::GFP remains uniformly dispersed (Figure 9). The double mutants,
630 *unc-5;madd-2,* are similar to the single *madd-2* mutant. Similar results are observed with *sax-3*
631 and *unc-5;sax-3* mutants (Figure 9). We hypothesize that in the *madd-2* and *sax-3* mutations the
632 degree to which the direction of UNC-40 localization fluctuates is so great that the *unc-5*
633 mutation makes no difference on the UNC-40::GFP clustering phenotype.

634

635 We suggest these results support our model in which UNC-40-mediated outgrowth is an
636 independent process that is coupled to the SOAL process in the HSN neuron. Previously we
637 hypothesized that UNC-40 SOAL is a general cellular process that polarizes and orients cellular
638 activities to the surrounding environment (YANG *et al.* 2014). In neurons during the
639 development of axons, UNC-40 SOAL is coupled to the outgrowth machinery. However, UNC-40
640 SOAL may also become coupled to other cellular activities. For example, UNC-6, UNC-5, and

641 UNC-40 are also known to play a role in localizing synapses in neurons (COLON-RAMOS *et al.*
642 2007; POON *et al.* 2008; KILLEEN 2009).

643

644 **Discussion**

645 In this paper, we show that UNC-5 regulates the number and length of neuronal processes that
646 a neuron can develop. We observe that *unc-5* loss-of-function mutations inhibit the
647 development of multiple neurites during early outgrowth from HSN. They also suppress the
648 development of extra HSN processes that are induced by a *mig-15* mutation or by expression of
649 the N-terminal fragment of UNC-6. We also observe that *unc-5* mutations suppress the anterior
650 overextension of the PLM axon that occurs in the *mig-15* mutant. Finally, in combination with
651 the *mig-15* mutation, *unc-5* loss-of-function mutations affect the branching and extension of
652 ALM and AVM axons at the nerve ring. In each of these cases, the pattern of outgrowth is
653 altered by loss of UNC-5 function. We further show that UNC-5 acts together with UNC-6, EGL-
654 20, SAX-3, UNC-53, MIG-15, and MADD-2 to regulate UNC-40 asymmetric localization at a
655 surface of HSN. Here we discuss a model to explain how UNC-5 could control patterns of
656 outgrowth by regulating UNC-40 stochastically orientated asymmetric localization (SOAL).

657

658 **UNC-40 SOAL; a model to explain *unc-5* phenotypes**

659 We hypothesize that UNC-40 undergoes stochastically orientated asymmetric localization
660 (SOAL) within neurons. Because this is a stochastic process, there is a probability of UNC-40
661 localizing and mediating outgrowth at each surface of the neuron. The probability of outgrowth
662 at each point along a surface may vary. This means that at one instance of time there is a
663 probability that UNC-40-mediated outgrowth will occur in a specific direction from a point
664 along the surface of the neuron. At the next instance of time there is a probability that

665 outgrowth will not occur at this point, but will instead occur at another point and in a different
666 direction. When considered over time, the direction of outgrowth fluctuates. This type of
667 movement can be modeled as a random walk, and random walks predict that the displacement
668 of the membrane will depend on the degree to which the direction of outgrowth movement
669 fluctuates. Extracellular cues, and the neuron's response to these cues, set the probability of
670 outgrowth happening at each point along the surface and therefore regulate the amount of
671 fluctuation. The process occurs at the micro-scale and it controls the direction and rate of
672 outgrowth movement. Below we describe how this model can explain the patterns of
673 outgrowth extension seen in the *unc-5* mutants.

674

675 Figure 2 depicts the essential concepts underlying the explanations. The same depiction is used
676 to explain the mutant phenotypes in Figures 10-15. Four important concepts are presented by
677 these figures. (1) There are numerous extracellular cues acting on the neuron to set the
678 probability of outgrowth in each direction. These cues include secreted molecules, such as
679 UNC-6 and EGL-20, as well as many other cues, such as extracellular matrix components (YANG
680 *et al.* 2014). For movement in the anterior and posterior directions, the neuron's response to
681 the cues sets an equal probability for movement in the dorsal and ventral direction. For
682 movement in the dorsal and ventral directions, the neuron's response to the cues sets an equal
683 probability for movement in the anterior and posterior direction. These cues are depicted in
684 the figures as purple, blue, orange, and red color gradients. (2) Besides UNC-40-mediated
685 outgrowth activity, cues also set the probability of nonUNC-40-mediated outgrowth activity at
686 each surface of the neuron. For example, there is a high probability for anteriorly directed
687 outgrowth in *unc-40* mutants, indicating that the cues set a high probability for anterior
688 nonUNC-40-mediated activity in the mutants. In the figures, a high relative probability for
689 UNC-40-mediated or nonUNC-40-mediated outgrowth activity at a surface is depicted as red

690 and green areas, respectively. The colored area is concentrated when there is a high
691 probability for outgrowth in one direction, and the area is more diffuse when the probability
692 for outgrowth in directions perpendicular to the directional bias are greater. (3) As the
693 probability of outgrowth decreases in the direction of outgrowth, and the probability of
694 outgrowth in directions perpendicular to the directional bias become greater, the extent of
695 movement forward decreases. This idea is based on random walk modeling. Representative
696 modeling is shown above or to the side of each diagram. 50 random walks from a point on a
697 line were calculated based on the given probabilities. As the probability for movement in
698 directions perpendicular to the directional bias become greater, the extent of movement from
699 the origin decreases. Similarly, we hypothesize that the forward displacement of the
700 membrane decreases as the probability for perpendicular outgrowth movement become
701 greater at the surface of the neuronal membrane. (4) Loss of UNC-5 function causes a higher
702 probability of UNC-40 mediating outgrowth in directions perpendicular to the directional bias.
703 Loss of MIG-15 reduces the probability of UNC-40-mediated outgrowth in directions
704 perpendicular to the directional bias. These ideas are based on our observations of the effects
705 that *unc-5* and *mig-15* mutations have on HSN localization of UNC-40::GFP and the direction of
706 HSN outgrowth. We further speculate that loss of MIG-15 function increases the probability of
707 nonUNC-40-mediated outgrowth in directions perpendicular to the directional bias. This is
708 based on our observation that HSN tends to be bipolar in the *mig-15* mutant (YANG *et al.* 2014),
709 suggesting that nonUNC-40-mediated outgrowth activity, which drives outgrowth anteriorly in
710 other mutants, becomes ineffectual.

711

712 **PLM extension phenotype:** We hypothesize that there is high probability for anteriorly
713 directed outgrowth from the PLM cell body because of the strong effect of a cue(s) which
714 inhibits outgrowth activity and is present in high concentration posterior to the cell body

715 (Figure 10A, position 1). Dorsal and ventral cues create an equal probability for dorsal and
716 ventral outgrowth, allowing the UNC-40 SOAL process to cause a high probability for anterior
717 outgrowth activity (Figure 10B, position 1). At a position that is further anterior (Figure 10A,
718 position 2), the inhibitory effect of another cue reduces the probability for anterior outgrowth
719 activity, while increasing the probability of outgrowth in the dorsal and ventral directions. This
720 does not affect the anterior bias for outgrowth, although it may affect the rate of outgrowth
721 (Figure 10B, position 2). Cues at an anterior position (Figure 10A, position 3), strongly inhibit
722 outgrowth and cause a greater probability of outgrowth in the dorsal and ventral directions
723 (Figure 10B, position 3). This arrests forward outgrowth. However, in some mutants the
724 inhibitory effect of these cues is not as great, allowing a stronger anterior bias at position 3. As
725 the outgrowth passes this position (Figure 10A, position 4), a situation similar to position 1 is
726 reestablished (Figure 10B, position 4).

727

728 We propose that PLM termination and overextension is influenced by the degree to which UNC-
729 40-mediated outgrowth fluctuates at position 3 (Figure11). In wildtype, the cues cause the
730 direction of both UNC-40-mediated and nonUNC-40-mediated outgrowth to fluctuate, resulting
731 in outgrowth stalling. Loss of UNC-40 function will not alter this. Loss of MIG-15 function
732 increases the probability of anterior UNC-40-mediated outgrowth by decreasing the degree to
733 which the direction of UNC-40-mediated outgrowth fluctuates. This allows a stronger anterior
734 directional bias, which results in the overextension phenotype. Loss of UNC-5 suppresses the
735 overextension caused by loss of MIG-15 function by increasing the degree to which the
736 direction of UNC-40-mediated outgrowth fluctuates, reverting the state back towards
737 wildtype.

738

739 **ALM and AVM nerve ring branching and extension phenotype:** We hypothesize that at the
740 nerve ring there are cues, including UNC-6, that are arranged along the dorsal/ventral axis.
741 These cues can promote ALM and AVM axon outgrowth. As an extension nears the nerve ring,
742 these cues help create a high probability for anterior outgrowth (Figure 12A and 12B, position
743 1). At the nerve ring, the cues create an equal probability for anterior outgrowth and
744 outgrowth into the ring (Figure 12A and 12B, position 2). Outgrowth extends into the nerve
745 ring because the cues of the nerve ring promote outgrowth and because the cues anterior and
746 posterior to the ring set an equal probability of outgrowth in those directions (Figure 12A and
747 12B, position 3). Outgrowth can also extend anteriorly from the nerve ring if cues anterior to
748 position 2 also promote outgrowth and cues dorsal and ventral create an equal probability of
749 outgrowth in those directions (Figure 12A and 12B, position 4).

750

751 We propose that ALM and AVM nerve ring branching and extension at the nerve ring is
752 influenced by the degree to which UNC-40-mediated outgrowth fluctuates at position 2 (Figure
753 13). In wildtype, the nerve ring cues create a higher probability for UNC-40-mediated
754 outgrowth into the nerve ring. In UNC-40 mutants, the axons often fail to branch into the nerve
755 ring but they still project further anterior, suggesting that the probability for anterior nonUNC-
756 40-mediated outgrowth is high in the *unc-40* mutant. Loss of MIG-15 function does not affect
757 the branching and extension because the higher probability for UNC-40-mediated outgrowth
758 activity remains. In *unc-40;mig-15* mutants, there is extension in both directions because loss
759 of MIG-15 function increases the probability of nonUNC-40-mediated outgrowth in other
760 directions and the nonUNC-40-mediated outgrowth allows outgrowth into the nerve ring. In
761 *unc-5;mig-15* mutants, the direction of both UNC-40-mediated and nonUNC-40-mediated
762 outgrowth fluctuate, causing outgrowth stalling in each direction. In these mutants, there is
763 often an absence of extension both anteriorly and into the nerve ring.

764

765 **HSN extension phenotypes:** We hypothesize that there is high probability for ventrally
766 directed outgrowth from the HSN cell body because of the strong outgrowth-promoting effect
767 of the UNC-6 cue, which is in a higher concentration ventral of the cell body (Figure 14A,
768 position 1). Anterior and posterior cues create an equal probability for anterior and posterior
769 outgrowth, and there is a high probability for ventral outgrowth activity. As an extension
770 moves ventrally it encounters higher levels of the UNC-6 cue. The probability of outgrowth
771 towards the UNC-6 source increases, while the probabilities of outgrowth in the anterior and
772 posterior decrease (Figure 14B, positions 2). However, as the level of UNC-6 saturates the
773 receptors the probability for outgrowth in different directions increases, causing outward
774 movement to stall (Figure 14B, positions 3). The distance from the source of the cue at which
775 this happens is a function of the concentration of the cues, and the cell's ability to interact and
776 respond to the cues. If the cell's response to the UNC-6 cue causes a lower probability of
777 ventral outgrowth than in wildtype, the probabilities of anterior and posterior outgrowth will
778 be greater (Figure 14B, positions 1, right column). The greater fluctuation will slow the rate of
779 outgrowth as extension proceeds (Figure 14B, positions 2, right column). Again, at the source
780 of the cue the response may become saturated and outward movement will stall (Figure 14B,
781 positions 3, right column). In this scenario, the rate of outgrowth decreases, while the direction
782 of outgrowth is the same.

783

784 We propose that HSN extension is influenced by the degree to which UNC-40-mediated
785 outgrowth fluctuates. In wildtype, UNC-40-mediated outgrowth creates a high probability for
786 the initial ventral outgrowth (Figure 15A, top). Loss of UNC-5 function causes a higher
787 probability of UNC-40 mediating outgrowth in the anterior and posterior directions, and

788 consequently a decrease in the rate of outgrowth (Figure 15A, second from top). We suggest
789 this underlies the observation that extensions fail to form in the L1 stage in *unc-5* mutants, but
790 do form over time, and in the same direction, as in wild-type animals.

791

792 We also propose that controlling the degree to which the direction of UNC-40-mediated
793 outgrowth fluctuates at points along the surface can regulate the number of processes that
794 form. We suggest that UNC-40 (DCC), UNC-5 (UNC5), and UNC-6 (netrin) are part of an activator-
795 inhibitor system (GIERER AND MEINHARDT 1972; MEINHARDT AND GIERER 2000). In an activator-
796 inhibitor system two substances act on each other. The activator stimulates its own production as
797 well as produces an inhibitor that can repress the production of the activator. The inhibitor is able to
798 diffuse more rapidly than the activator, which causes patterns of varying concentrations of activator
799 and inhibitor. Pattern formation through local symmetry breaking, signal amplification, and long-
800 range inhibition may involve chemical, mechanical, or coupled mechanochemical processes
801 (GOEHRING AND GRILL 2013).

802

803 We suggest an activator-inhibitor system in which UNC-40 and UNC-5 are the two substances
804 that interact with each other (Figure 15B). This is consistent with evidence indicating that
805 Netrin-1 binds simultaneously to two DCC (UNC-40) molecules or an UNC5/DCC complex (FINCI
806 *et al.* 2014). In the context of an activator-inhibitor system, UNC-5 signaling acts as an activator
807 and UNC-40 signaling acts as an inhibitor. The activator and inhibitor activities "diffuse" at
808 different rates because recruitment of UNC-40 and UNC-5 to the plasma membrane occurs at
809 different rates. This idea is consistent with imaging experiments of cells in culture which
810 suggest that netrin-1 (UNC-6) regulates the distribution of DCC (UNC-40) and UNC5B (UNC-5)
811 at the plasma membrane (GOPAL *et al.* 2016). In these studies, netrin-1 (UNC-6) was shown to
812 stimulate translocation of DCC (UNC-40) and UNC5B (UNC-5) receptors from intracellular

813 vesicles to the plasma membrane and, further, the transported receptors were shown to
814 localize at the plasma membrane (GOPAL *et al.* 2016).
815
816 We propose that signaling by UNC-6-ligated UNC-40 causes outgrowth activity and stimulates
817 translocation of UNC-40 to the site (Figure 15B, step 1). If the outgrowth reaches a critical
818 level of UNC-6 (Figure 15B, step 2), changes to the UNC-6/UNC-40/UNC-5 receptor complexes
819 increase UNC-5 signaling. UNC-5 signaling inhibits UNC-40 translocation to the site and
820 increases the relative levels of UNC-5 (short-range autocatalytic). Locally, UNC-40-mediated
821 outgrowth activity becomes more dispersed, resulting in a slower rate of outgrowth. As UNC-
822 40 translocation to the leading edge is inhibited, the relative levels of UNC-40 at flanking
823 surfaces increases (Figure 15B, step 3). These UNC-40 levels inhibit UNC-5 signaling (long-
824 range inhibition) and prevent the dispersion of UNC-40-mediated outgrowth activity, resulting
825 in a faster rate of outgrowth at the flanking surfaces. In the context of an activator-inhibitor
826 system, UNC-5 signaling functions as an activator because it stimulates its own activity by
827 decreasing the ratio of UNC-40 to UNC-5 at the site of UNC-5 signaling. It also stimulates
828 production of UNC-40 UNC-5-inhibitory activity by increasing the ratio of UNC-40 to UNC-5 at
829 the flanking regions. As the flanking regions move further outward due to the UNC-40-
830 mediated outgrowth activity, UNC-40 translocation to the surface is further stimulated by
831 increasing levels of the extracellular UNC-6 cue.
832
833 In this type of model, the reaction and diffusion rates of the substances influence the pattern
834 that emerges. In the above example, whether the flanking areas branch further depends on
835 whether the critical level of receptors and extracellular ligands is realized at the flanking
836 region. The *mig-15(rh148)* mutation and the expression of UNC-6ΔC could alter the rate by
837 which components of the UNC-6/UNC-40/UNC-5 receptor complexes interact or could alter the

838 rate of translocation of the components to the membrane, or both. In fact, cell culture
839 experiments suggest Netrin VI-V (UNC-6ΔC) induces DCC and UNC5B colocalization, but not
840 DCC recruitment (GOPAL *et al.* 2016). Moreover, mutations that suppress ectopic branching
841 induced by UNC-6ΔC expression affect members of second messenger systems which could
842 influence the rates of UNC-40 and UNC-5 interactions and trafficking (WANG AND WADSWORTH
843 2002).

844

845 **A genetic pathway for UNC-40 asymmetric localization**

846 We present a genetic pathway for the asymmetrical localization of UNC-40 based on the phenotype
847 of robust UNC-40::GFP clustering in HSN. It is worth noting that the SOAL model of axon
848 outgrowth does not depend on knowledge of the molecular mechanisms of outgrowth. Rather,
849 the SOAL model uses a statistical approach to understand how a gene influences the collective
850 impact of all the underlying molecular mechanisms that drives outgrowth. It can be envisioned
851 that the movement of an extension occurs through innumerable forces acting at the molecular
852 level. The effect that each molecular event has on movement is not easily observed or
853 measured. In fact, it may be that patterns of outgrowth can't be fully understood by only
854 knowing the molecular mechanisms of outgrowth. Instead, the effects that molecular events
855 collectively have on movement must be understood through a statistical model.

856

857 Nevertheless, a full understanding of the molecular mechanisms underlying the SOAL process is
858 an important long-term goal. Since we believe that UNC-40::GFP clustering is a readout of that
859 process, constructing genetic pathways for the clustering of UNC-40::GFP is a step toward this
860 goal. We wish to know how UNC-5 mediates signaling within HSN that controls the UNC-40
861 asymmetric localization process. However, a role for UNC-5 in HSN is paradoxical given the

862 widespread idea that UNC-5 mediates a repulsive response to UNC-6 and that HSN outgrowth is
863 towards the source of UNC-6. All the same, we suggest a cell-autonomous role for UNC-5 in
864 HSN is the most parsimonious model. First, UNC-5 is an UNC-6 receptor that can mediate
865 neuronal responses when in complex with UNC-40 (HONG *et al.* 1999; GEISBRECHT *et al.* 2003;
866 KRUGER *et al.* 2004; FINCI *et al.* 2014). We previously showed that UNC-40 conformational
867 changes regulate HSN asymmetric localization in HSN (XU *et al.* 2009) and we now show that
868 UNC-5 regulates UNC-40 asymmetric localization in HSN. It is therefore plausible that UNC-5
869 affects UNC-40 conformational changes that regulate UNC-40 asymmetric localization. Second,
870 UNC-5 can alter the number to HSN outgrowths in response to UNC-6 and to the UNC-6ΔC
871 ligand. Directional guidance by UNC-6 and UNC-6ΔC is generally normal in an *unc-5* mutant,
872 suggesting that the ability of UNC-5 to regulate the number of outgrowth is not due to an
873 alteration in the extracellular distribution of its UNC-6 ligand. Further, the UNC-6ΔC ligand and
874 the *mig-15* mutation create the same outgrowth phenotype, which can be suppressed by loss of
875 UNC-5 function, and we have shown that MIG-15 acts cell autonomously in HSN to regulate
876 UNC-40 asymmetric localization (YANG *et al.* 2014). Further, we have shown that the UNC-5-
877 mediated response that regulates UNC-40 asymmetric localization also depends on UNC-53
878 (NAV2) (KULKARNI *et al.* 2013), a cytoplasmic protein that functions cell-autonomously for cell
879 migration and axon guidance (STRINGHAM *et al.* 2002). Together, these observations strongly
880 suggest that UNC-5 directly regulates signaling within HSN. Third, a role for UNC-5 in the
881 guidance of AVM and PVM axons towards UNC-6 sources has also been suggested. A synergistic
882 interaction between *unc-5* and *egl-20* is observed; in either *unc-5* or *egl-20* mutants the ventral
883 extension of AVM and PVM axons is only slightly impaired, whereas in the double mutants
884 there is a much greater penetrance (LEVY-STRUMPF AND CULOTTI 2014). The expression of an *unc-*
885 *5* transgene in AVM and PVM can rescue the AVM and PVM axon guidance defects of the *unc-*
886 *5;egl-20* double mutant (LEVY-STRUMPF AND CULOTTI 2014). We note that for HSN, transgenic

887 rescue using *unc-5* constructs have not been successful and in wild-type animals UNC-5
888 expression in HSN has not been reported. As well, expression has not been reported in AVM,
889 PVM, and PLM wild-type neurons. We suspect there may be technical difficulties or that UNC-5
890 expression might be low in these cells. UNC-5 is detected in PLM in *rpm-1* mutants, which is
891 consistent with evidence that UNC-5 activity is required for PLM overextension in these
892 mutants (Li *et al.* 2008).

893

894 To construct genetic pathways, we use the readout of whether UNC-40::GFP is clearly and
895 consistently localized to any side of the HSN neuron in different mutants (Figure 9). A
896 summary of the results is presented (Figure 16A). UNC-6 is required for robust asymmetric
897 UNC-40 localization; in the absence of UNC-6 function UNC-40 remains uniformly distributed
898 along the surface of the plasma membrane. The loss of both UNC-53 and UNC-5 function also
899 results in a uniform distribution, however loss of either one alone does not. This suggests that
900 UNC-53 and UNC-5 pathways act redundantly downstream of UNC-6 (Figure 16B). Moreover,
901 we observe there is robust asymmetric UNC-40 localization when there is a loss of UNC-6
902 activity in addition to the loss of UNC-53 and UNC-5. This suggests a third pathway that is
903 suppressed by UNC-6 when UNC-53 and UNC-5 activity are missing. Loss of both UNC-5 and
904 UNC-6 does not allow UNC-40 localization, whereas loss of both UNC-53 and UNC-6 does,
905 therefore UNC-53, rather than UNC-5, acts with UNC-6 to suppress the third pathway.

906

907 UNC-40 becomes localized when EGL-20 activity is lost. As well, UNC-40 becomes localized
908 when both EGL-20 and UNC-53 activities are lost. This is consistent with UNC-6 promoting
909 UNC-40 localization via the UNC-5 pathway. Loss of EGL-20 and UNC-5 prevents UNC-40
910 localization. In these animals, the UNC-5 pathway is absent and UNC-6 is present to blocks the

911 third pathway, therefore the UNC-53 pathway that leads to UNC-40 localization must require
912 EGL-20, as well as UNC-6.
913
914 Loss of UNC-6 activity or loss of both UNC-6 and EGL-20 activity prevents localization, whereas
915 loss of only EGL-20 does not. To explain this, we propose that when UNC-6 is lost, the third
916 pathway, which would otherwise be activated by the loss of UNC-6, remains suppressed
917 because EGL-20 activity promotes suppression via UNC-53 activity. This suppression also
918 explains why loss of UNC-6 and UNC-5 activity does not cause localization.
919
920 Importantly, this genetic analysis indicates that netrin (UNC-6) and wnt (EGL-20) signaling are
921 integrated to regulate self-organizing UNC-40 asymmetric localization. An implication of this
922 result is that the extracellular concentrations of UNC-6 and EGL-20 could control the activation
923 or inhibition of UNC-40-mediated outgrowth. This could be important for generating patterns
924 of outgrowth when neurons move to new locations within the animal. The picture is
925 complicated by the evidence that both UNC-6 and EGL-20 affect the SOAL of both UNC-40-
926 mediated and nonUNC-40-mediated outgrowth activity. It is possible that overlapping sets of
927 extracellular cues and their receptors are involved in setting the probability of outgrowth for
928 each activity. SAX-3 and MADD-2 are required for UNC-40::GFP localization, but also affect
929 nonUNC-40-mediated outgrowth. The *egl-20;sax-3* and *unc-40;sax-3* double mutations have the
930 greatest effect on restricting the extent of outgrowth movement in any direction (Figures 6 and
931 7). Moreover, the number of HSN neurites is reduced in *unc-5* mutants, whereas the number in
932 *unc-5;sax-3* double mutants appears normal (Figure 3B). Understanding the interdependence
933 of these outgrowth activities will be necessary for better understand how extracellular cues
934 affect the patterns of outgrowth *in vivo*.
935

936 **Acknowledgments**

937 We thank Caenorhabditis Genetics Center, J. Culotti, and C. Bargmann for strains; we thank
938 Martha Soto and members of the Soto laboratory for support and helpful discussions; we thank
939 Bhumi Patel and Leely Rezvani for comments on the manuscript. This work was supported by
940 grants NS033156 and NS061805 from the National Institutes of Health, National Institute of
941 Neurological Disorders and Stroke and grant 07-3060-SCR-E-0 from the New Jersey
942 Commission on Spinal Cord to WGW. This work was also supported by grant DFHS13PPCO28
943 from the New Jersey Commission on Cancer Research to AM.

944 Table

945

946

Table 1. Direction of Axon Formation from the HSN Cell Body

	direction of axon protrusion						
	dorsal	ventral	anterior	posterior	multipolar		
	%	%	%	%	%	*n*	reference
wildtype	0	96±2	3±2	0	1±1	221	(KULKARNI *et al.* 2013)
unc-6(ev400)	2±2	3±2	81±2	8±2	6±1	218	(KULKARNI *et al.* 2013)
unc-40(e1430)	2±1	6±2	67±2	19±1	6±1	183	(KULKARNI *et al.* 2013)
unc-5(e53)	0	75±3	19±2	1±1	5±1	245	(YANG *et al.* 2014)
unc-53(n152)	0	67±3	22±2	5±1	6±1	238	(KULKARNI *et al.* 2013)
sax-3(ky123)	2±1	31±1	21±1	37±2	9±2	232	(TANG AND WADSWORTH 2014)
*sax-3(ky200)**	2±1	32±1	19±2	42±3	5±2	198	(TANG AND WADSWORTH 2014)
unc-5(e53);sax-3(ky200)	2±1	40±3	24±2	28±2	6±1	120	
unc-5(e53);unc-6(ev400)	4±2	5±3	59±4	22±4	9±1	201	
unc-5(e53);egl-20(n585)	3±1	28±4	22±4	35±5	11±2	114	
unc-53(n152);unc-5(e53)	0	19±1	62±2	17±1	3±1	224	(KULKARNI *et al.* 2013)
unc-53(n152);unc-6(ev400)	24±2	0	19±2	22±2	34±3	144	(KULKARNI *et al.* 2013)
unc-53(n152);sax-3(ky123)	1±1	47±3	24±2	23±5	6±3	207	(TANG AND WADSWORTH 2014)
unc-40(e1430);unc-5(e53)	5±1	6±1	55±2	19±2	14±1	196	(KULKARNI *et al.* 2013)
*unc-40(e1430);sax-3(ky200)**	14±3	2±1	40±2	35±3	9±4	191	(TANG AND WADSWORTH 2014)
sax-3(ky200); unc-6(ev400)*	8±1	8±2	49±3	20±5	14±2	211	(TANG AND WADSWORTH 2014)
unc-53(n152);unc-5(e53);unc-6(ev400)	23±2	0	34±2	15±2	28±2	148	(KULKARNI *et al.* 2013)
unc-53(n152);sax-3(ky200);unc-6(ev400)*	11±2	2±1	33±4	30±3	25±5	189	
egl-20(n585)	0	64±2	21±2	7±1	8±1	304	(TANG AND WADSWORTH 2014)
egl-20(n585); unc-6(ev400)	18±2	0	43±2	15±2	24±2	205	(TANG AND WADSWORTH 2014)
unc-40(e1430); egl-20(n585)	6±2	17±2	45±5	15±2	16±2	173	(TANG AND WADSWORTH 2014)
egl-20(n585);sax-3(ky123)	1±1	12±2	39±2	39±1	8±3	177	(TANG AND WADSWORTH 2014)
madd-2(tr103)	0	19±2	55±5	17±4	8±2	179	
madd-2(ky592)	0	52±2	43±2	5±1	0	95	
unc-5(e53);madd-2(tr103)	3±1	15±2	52±4	17±4	13±1	197	
madd-2(tr103);sax-3(ky123)	2	24±3	19±4	47±1	7±2	171	
unc-53(n152);madd-2(tr103)	1±1	15±2	43±2	17±1	24±4	148	
mig-15(rh326)	2±1	15±1	24±3	11±3	48±8	131	(YANG *et al.* 2014)

Numbers represent percentage value ± SEM.

*Animals grown at the *sax-3(ky200)* restrictive temperature (25°C).

947

948 **References**

949 Adler, C. E., R. D. Fetter and C. I. Bargmann, 2006 UNC-6/Netrin induces neuronal asymmetry and
950 defines the site of axon formation. Nat Neurosci 9**:** 511-518.

951 Aiello, G. L., 2016 Neuro-Percolation as a Superposition of Random-Walks, pp. in *European*
952 *Symposium on Artificial Neural Networks, Computational Intelligence and Machine Learning*.
953 i6doc.com Bruges, Belgium.

954 Alexander, M., K. K. Chan, A. B. Byrne, G. Selman, T. Lee *et al.*, 2009 An UNC-40 pathway directs
955 postsynaptic membrane extension in Caenorhabditis elegans. Development 136**:** 911-922.

956 Alexander, M., G. Selman, A. Seetharaman, K. K. Chan, S. A. D'Souza *et al.*, 2010 MADD-2, a
957 homolog of the Opitz syndrome protein MID1, regulates guidance to the midline through UNC-40 in
958 Caenorhabditis elegans. Developmental Cell 18**:** 961-972.

959 Asakura, T., K. Ogura and Y. Goshima, 2007 UNC-6 expression by the vulval precursor cells of
960 Caenorhabditis elegans is required for the complex axon guidance of the HSN neurons. Dev Biol
961 304**:** 800-810.

962 Chan, S. S., H. Zheng, M. W. Su, R. Wilk, M. T. Killeen *et al.*, 1996 UNC-40, a C. elegans homolog
963 of DCC (Deleted in Colorectal Cancer), is required in motile cells responding to UNC-6 netrin cues.
964 Cell 87**:** 187-195.

965 Chang, C., C. E. Adler, M. Krause, S. G. Clark, F. B. Gertler *et al.*, 2006 MIG-10/Lamellipodin and
966 AGE-1/PI3K Promote Axon Guidance and Outgrowth in Response to Slit and Netrin. Curr Biol 16**:**
967 854-862.

968 Chapman, J. O., H. Li and E. A. Lundquist, 2008 The MIG-15 NIK kinase acts cell-autonomously in
969 neuroblast polarization and migration in C. elegans. Dev Biol 324**:** 245-257.

970 Colavita, A., and J. G. Culotti, 1998 Suppressors of ectopic UNC-5 growth cone steering identify
971 eight genes involved in axon guidance in Caenorhabditis elegans. Dev Biol 194**:** 72-85.

972 Colon-Ramos, D. A., M. A. Margeta and K. Shen, 2007 Glia promote local synaptogenesis through
973 UNC-6 (netrin) signaling in C. elegans. Science 318**:** 103-106.

974 Finci, L. I., N. Krüger, X. Sun, J. Zhang, M. Chegkazi *et al.*, 2014 The crystal structure of netrin-1 in
975 complex with DCC reveals the bifunctionality of netrin-1 as a guidance cue. Neuron 83**:** 839-849.

976 Geisbrecht, B. V., K. A. Dowd, R. W. Barfield, P. A. Longo and D. J. Leahy, 2003 Netrin binds
977 discrete subdomains of DCC and UNC5 and mediates interactions between DCC and heparin. J Biol
978 Chem 278**:** 32561-32568.

979 Gierer, A., and H. Meinhardt, 1972 A theory of biological pattern formation. Kybernetik 12**:** 30-39.

980 Goehring, N. W., and S. W. Grill, 2013 Cell polarity: mechanochemical patterning. Trends Cell Biol
981 23**:** 72-80.

982 Gopal, A. A., B. Rappaz, V. Rouger, I. B. Martyn, P. D. Dahlberg *et al.*, 2016 Netrin-1-Regulated
983 Distribution of UNC5B and DCC in Live Cells Revealed by TICCS. Biophys J 110**:** 623-634.

984 Hagedorn, E. J., J. W. Ziel, M. A. Morrissey, L. M. Linden, Z. Wang *et al.*, 2013 The netrin receptor
985 DCC focuses invadopodia-driven basement membrane transmigration in vivo. J Cell Biol 201**:** 903-
986 913.

987 Hao, J. C., C. E. Adler, L. Mebane, F. B. Gertler, C. I. Bargmann *et al.*, 2010 The tripartite motif
988 protein MADD-2 functions with the receptor UNC-40 (DCC) in Netrin-mediated axon attraction and
989 branching. Dev Cell 18**:** 950-960.

990 Hao, J. C., T. W. Yu, K. Fujisawa, J. G. Culotti, K. Gengyo-Ando *et al.*, 2001 C. elegans Slit Acts in
991 Midline, Dorsal-Ventral, and Anterior-Posterior Guidance via the SAX-3/Robo Receptor. Neuron 32**:**
992 25-38.

993 Hedgecock, E. M., J. G. Culotti and D. H. Hall, 1990 The unc-5, unc-6, and unc-40 genes guide
994 circumferential migrations of pioneer axons and mesodermal cells on the epidermis in C. elegans.
995 Neuron 4**:** 61-85.

996 Hong, K., L. Hinck, M. Nishiyama, M. M. Poo, M. Tessier-Lavigne *et al.*, 1999 A ligand-gated
997 association between cytoplasmic domains of UNC5 and DCC family receptors converts netrin-
998 induced growth cone attraction to repulsion. Cell 97**:** 927-941.

999 Keleman, K., and B. J. Dickson, 2001 Short- and long-range repulsion by the Drosophila Unc5 netrin
1000 receptor. Neuron 32**:** 605-617.

1001 Killeen, M., J. Tong, A. Krizus, R. Steven, I. Scott *et al.*, 2002 UNC-5 function requires
1002 phosphorylation of cytoplasmic tyrosine 482, but its UNC-40-independent functions also require a
1003 region between the ZU-5 and death domains. Dev Biol 251**:** 348-366.

1004 Killeen, M. T., 2009 The dual role of the ligand UNC-6/Netrin in both axon guidance and
1005 synaptogenesis in C. elegans. Cell Adh Migr 3**:** 268-271.

1006 Kruger, R. P., J. Lee, W. Li and K. L. Guan, 2004 Mapping netrin receptor binding reveals domains
1007 of Unc5 regulating its tyrosine phosphorylation. J Neurosci 24**:** 10826-10834.

1008 Kulkarni, G., Z. Xu, A. M. Mohamed, H. Li, X. Tang *et al.*, 2013 Experimental evidence for UNC-6
1009 (netrin) axon guidance by stochastic fluctuations of intracellular UNC-40 (DCC) outgrowth activity.
1010 Biol Open 2**:** 1300-1312.

1011 Lai Wing Sun, K., J. P. Correia and T. E. Kennedy, 2011 Netrins: versatile extracellular cues with
1012 diverse functions. Development 138**:** 2153-2169.

1013 Leung-Hagesteijn, C., A. M. Spence, B. D. Stern, Y. Zhou, M. W. Su *et al.*, 1992 UNC-5, a
1014 transmembrane protein with immunoglobulin and thrombospondin type 1 domains, guides cell and
1015 pioneer axon migrations in C. elegans. Cell 71**:** 289-299.

1016 Levy-Strumpf, N., and J. G. Culotti, 2014 Netrins and Wnts function redundantly to regulate antero-
1017 posterior and dorso-ventral guidance in C. elegans. PLoS Genet 10**:** e1004381.

1018 Li, H., G. Kulkarni and W. G. Wadsworth, 2008 RPM-1, a Caenorhabditis elegans protein that
1019 functions in presynaptic differentiation, negatively regulates axon outgrowth by controlling SAX-
1020 3/robo and UNC-5/UNC5 activity. J Neurosci 28**:** 3595-3603.

1021 Lim, Y. S., S. Mallapur, G. Kao, X. C. Ren and W. G. Wadsworth, 1999 Netrin UNC-6 and the
1022 regulation of branching and extension of motoneuron axons from the ventral nerve cord of
1023 Caenorhabditis elegans. J Neurosci 19**:** 7048-7056.

1024 MacNeil, L. T., W. R. Hardy, T. Pawson, J. L. Wrana and J. G. Culotti, 2009 UNC-129 regulates the
1025 balance between UNC-40 dependent and independent UNC-5 signaling pathways. Nat Neurosci 12**:**
1026 150-155.

1027 Maes, T., A. Barcelo and C. Buesa, 2002 Neuron navigator: a human gene family with homology to
1028 unc-53, a cell guidance gene from Caenorhabditis elegans. Genomics 80**:** 21-30.

1029 Manser, J., C. Roonprapunt and B. Margolis, 1997 C. elegans cell migration gene mig-10 shares
1030 similarities with a family of SH2 domain proteins and acts cell nonautonomously in excretory canal
1031 development. Dev Biol 184**:** 150-164.

1032 Manser, J., and W. B. Wood, 1990 Mutations affecting embryonic cell migrations in Caenorhabditis
1033 elegans. Dev Genet 11**:** 49-64.

1034 McShea, M. A., K. L. Schmidt, M. L. Dubuke, C. E. Baldiga, M. E. Sullender *et al.*, 2013 Abelson
1035 interactor-1 (ABI-1) interacts with MRL adaptor protein MIG-10 and is required in guided cell
1036 migrations and process outgrowth in C. elegans. Dev Biol 373**:** 1-13.

1037 Meinhardt, H., and A. Gierer, 2000 Pattern formation by local self-activation and lateral inhibition.
1038 Bioessays 22**:** 753-760.

1039 Merz, D. C., H. Zheng, M. T. Killeen, A. Krizus and J. G. Culotti, 2001 Multiple signaling
1040 mechanisms of the unc-6/netrin receptors unc-5 and unc-40/dcc in vivo. Genetics 158**:** 1071-1080.

1041 Moore, S. W., M. Tessier-Lavigne and T. E. Kennedy, 2007 Netrins and their receptors. Adv Exp
1042 Med Biol 621**:** 17-31.

1043 Morikawa, R. K., T. Kanamori, K. Yasunaga and K. Emoto, 2011 Different levels of the Tripartite
1044 motif protein, Anomalies in sensory axon patterning (Asap), regulate distinct axonal projections of
1045 Drosophila sensory neurons. Proc Natl Acad Sci U S A 108**:** 19389-19394.

1046 Norris, A. D., and E. A. Lundquist, 2011 UNC-6/netrin and its receptors UNC-5 and UNC-40/DCC
1047 modulate growth cone protrusion in vivo in C. elegans. Development.

1048 Pan, C. L., J. E. Howell, S. G. Clark, M. Hilliard, S. Cordes *et al.*, 2006 Multiple Wnts and frizzled
1049 receptors regulate anteriorly directed cell and growth cone migrations in Caenorhabditis elegans. Dev
1050 Cell 10**:** 367-377.

1051 Poinat, P., A. De Arcangelis, S. Sookhareea, X. Zhu, E. M. Hedgecock *et al.*, 2002 A conserved
1052 interaction between beta1 integrin/PAT-3 and Nck-interacting kinase/MIG-15 that mediates
1053 commissural axon navigation in C. elegans. Curr Biol 12**:** 622-631.

1054 Poon, V. Y., M. P. Klassen and K. Shen, 2008 UNC-6/netrin and its receptor UNC-5 locally exclude
1055 presynaptic components from dendrites. Nature.

1056 Quinn, C. C., D. S. Pfeil, E. Chen, E. L. Stovall, M. V. Harden *et al.*, 2006 UNC-6/netrin and SLT-
1057 1/slit guidance cues orient axon outgrowth mediated by MIG-10/RIAM/lamellipodin. Curr Biol 16**:**
1058 845-853.

1059 Quinn, C. C., D. S. Pfeil and W. G. Wadsworth, 2008 CED-10/Rac1 mediates axon guidance by
1060 regulating the asymmetric distribution of MIG-10/lamellipodin. Curr Biol 18**:** 808-813.

1061 Ren, X. C., S. Kim, E. Fox, E. M. Hedgecock and W. G. Wadsworth, 1999 Role of netrin UNC-6 in
1062 patterning the longitudinal nerves of Caenorhabditis elegans. J Neurobiol 39**:** 107-118.

1063 Shakir, M. A., J. S. Gill and E. A. Lundquist, 2006 Interactions of UNC-34 Enabled with Rac
1064 GTPases and the NIK kinase MIG-15 in Caenorhabditis elegans axon pathfinding and neuronal
1065 migration. Genetics 172**:** 893-913.

1066 Song, S., Q. Ge, J. Wang, H. Chen, S. Tang *et al.*, 2011 TRIM-9 functions in the UNC-6/UNC-40
1067 pathway to regulate ventral guidance. Journal of genetics and genomics = Yi chuan xue bao 38**:** 1-11.

1068 Stringham, E., N. Pujol, J. Vandekerckhove and T. Bogaert, 2002 unc-53 controls longitudinal
1069 migration in C. elegans. Development 129**:** 3367-3379.

1070 Stringham, E. G., and K. L. Schmidt, 2009 Navigating the cell: UNC-53 and the navigators, a family
1071 of cytoskeletal regulators with multiple roles in cell migration, outgrowth and trafficking. Cell
1072 adhesion & migration 3**:** 342-346.

1073 Tang, X., and W. G. Wadsworth, 2014 SAX-3 (Robo) and UNC-40 (DCC) Regulate a Directional
1074 Bias for Axon Guidance in Response to Multiple Extracellular Cues. PLoS One 9**:** e110031.

1075 Tessier-Lavigne, M., and C. S. Goodman, 1996 The molecular biology of axon guidance. Science
1076 274**:** 1123-1133.

1077 Teulière, J., C. Gally, G. Garriga, M. Labouesse and E. Georges-Labouesse, 2011 MIG-15 and ERM-
1078 1 promote growth cone directional migration in parallel to UNC-116 and WVE-1. Development 138**:**
1079 4475-4485.

1080 Wadsworth, W. G., H. Bhatt and E. M. Hedgecock, 1996 Neuroglia and pioneer neurons express
1081 UNC-6 to provide global and local netrin cues for guiding migrations in C. elegans. Neuron 16**:** 35-
1082 46.

1083 Wadsworth, W. G., and E. M. Hedgecock, 1996 Hierarchical guidance cues in the developing
1084 nervous system of C. elegans. Bioessays 18**:** 355-362.

1085 Wang, Q., and W. G. Wadsworth, 2002 The C domain of netrin UNC-6 silences calcium/calmodulin-
1086 dependent protein kinase- and diacylglycerol-dependent axon branching in Caenorhabditis elegans. J
1087 Neurosci 22**:** 2274-2282.

1088 Wang, Z., Y. Hou, X. Guo, M. van der Voet, M. Boxem *et al.*, 2013 The EBAX-type Cullin-RING
1089 E3 ligase and Hsp90 guard the protein quality of the SAX-3/Robo receptor in developing neurons.
1090 Neuron 79**:** 903-916.

1091 Wang, Z., L. M. Linden, K. M. Naegeli, J. W. Ziel, Q. Chi *et al.*, 2014 UNC-6 (netrin) stabilizes
1092 oscillatory clustering of the UNC-40 (DCC) receptor to orient polarity. J Cell Biol 206**:** 619-633.

1093 Xu, Y., H. Taru, Y. Jin and C. C. Quinn, 2015 SYD-1C, UNC-40 (DCC) and SAX-3 (Robo) function
1094 interdependently to promote axon guidance by regulating the MIG-2 GTPase. PLoS Genet 11**:**
1095 e1005185.

1096 Xu, Z., H. Li and W. G. Wadsworth, 2009 The roles of multiple UNC-40 (DCC) receptor-mediated
1097 signals in determining neuronal asymmetry induced by the UNC-6 (netrin) ligand. Genetics 183:
1098 941-949.

1099 Yang, Y., W. S. Lee, X. Tang and W. G. Wadsworth, 2014 Extracellular Matrix Regulates UNC-6
1100 (Netrin) Axon Guidance by Controlling the Direction of Intracellular UNC-40 (DCC) Outgrowth
1101 Activity. PLoS One 9: e97258.

1102 Yoshimura, S., J. I. Murray, Y. Lu, R. H. Waterston and S. Shaham, 2008 mls-2 and vab-3 Control
1103 glia development, hlh-17/Olig expression and glia-dependent neurite extension in C. elegans.
1104 Development 135: 2263-2275.

1105 Zallen, J. A., B. A. Yi and C. I. Bargmann, 1998 The conserved immunoglobulin superfamily
1106 member SAX-3/Robo directs multiple aspects of axon guidance in C. elegans. Cell 92: 217-227.

1107 Ziel, J. W., E. J. Hagedorn, A. Audhya and D. R. Sherwood, 2009 UNC-6 (netrin) orients the
1108 invasive membrane of the anchor cell in C. elegans. Nat Cell Biol 11: 183-189.

1109

1110 **Figure 1. Model for UNC-40 self-organizing polarization and random walk movement.**
1111 (**A**) Along the plasma membrane, complexes comprising UNC-40 and UNC-5 interact with
1112 extracellular cues. A self-organizing process is triggered. In wild-type animals (top) there is a
1113 high probability that complexes associated with specific levels of the extracellular cues will
1114 mediate outgrowth activity. Compared to wildtype, in animals with loss of UNC-5 function
1115 (bottom) the probability of these same complexes mediating outgrowth activity is lower and
1116 the probability that the other complexes instead will mediate outgrowth is higher. Direction is
1117 labeled left, down, and right, in reference to the orientation of the figure and to emphasize that
1118 the model is not referring to any specific cues or their sources in the animal. (**B**) Two sets of
1119 tracks are shown to compare random walk models derived from representative wildtype and
1120 mutant experimental results. Compared to wildtype, the mutant has a lower probability of
1121 outgrowth in one specific direction (down) and a higher probability of outgrowth in other
1122 directions (left and right). Using the probability distributions shown below the tracks, 50
1123 simulated random walks of 500 steps were plotted from an origin. This comparison
1124 emphasizes that even though the direction of movement is the same, there is a difference in the
1125 average displacement. We propose this property of movement is manifested during neuronal
1126 extension in wildtype and mutant animals as a difference in the rate of outgrowth. In statistical
1127 physics, net movement through the action of random motion is diffusion. Here, each track
1128 models the trajectory that mass of the plasma membrane could move during extension. The
1129 probability density function of the position of the mass as a function of space and time is
1130 described by an advection-diffusion equation. In summary, we suggest that the advection-
1131 diffusion model can be used to describe the process by which mass at the leading edge of an
1132 extension is transported and that our results describe how genes regulate this transport.

1133

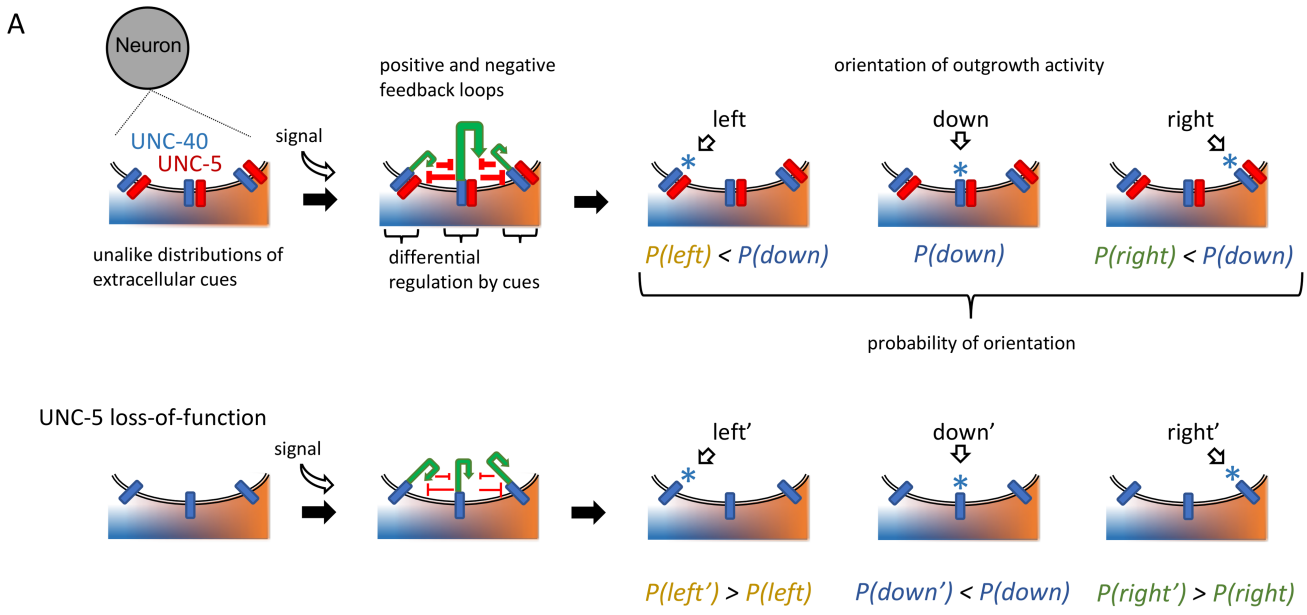

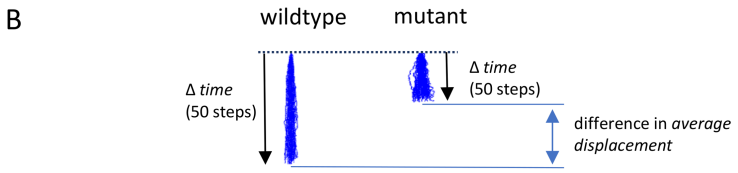

Example:						
	P(right)	=	0.1	0.33	=	*P(right')*
	P(left)	=	0.1	0.33	=	*P(left')*
	P(down)	=	0.8	0.33	=	*P(down')*

1136 **Figure 2. Model for outgrowth movement based on the SOAL model.** Schematic diagrams
1137 of the outgrowth of a neuron (gray) through an environment of multiple extracellular cues.
1138 These cues may be molecules presented at the surfaces of surrounding cells and extracellular
1139 matrix. The extracellular cues are represented here as color gradients of purple, blue, and
1140 orange. Outgrowth activity is mediated at the surface of the neuron through receptor activity.
1141 UNC-40-mediated activity is depicted in red, and nonUNC-40-mediated in green. The relative
1142 probability of activity along the surface is represented by the extent to which the colored areas
1143 cover the neuron's surface. Increasing the degree to which the direction of activity fluctuates
1144 over time decreases the extent of outward movement. Random walk models depicting this
1145 property are shown above each diagram. See text for details. **(A)** Depicted is the movement of
1146 a neuronal extension towards a source of a cue(s) (orange). At time 1 (top) the probability of
1147 outgrowth towards the source is high, however at time 2 (bottom) the probability of outgrowth
1148 in other directions increases as more receptors away from the leading edge are stimulated due
1149 to the higher concentration of the cue. This increases the degree to which the direction of
1150 activity fluctuates over time and decreases the extent of outward movement. **(B)** Depicted is
1151 the movement of a neuronal extension in wildtype (top) and an *unc-5* mutant (bottom). Loss of
1152 UNC-5 affects the UNC-40 SOAL process and causes more receptor activity away from the
1153 leading edge, thus decreasing the probability of outgrowth towards the source and increasing
1154 the probability of outgrowth in other directions. This increases the degree to which the
1155 direction of activity fluctuates over time and decreases the extent of outward movement.
1156 Under the same conditions, the rate of outward movement is reduced in *unc-5* mutants as
1157 compared to wildtype.
1158
1159
1160

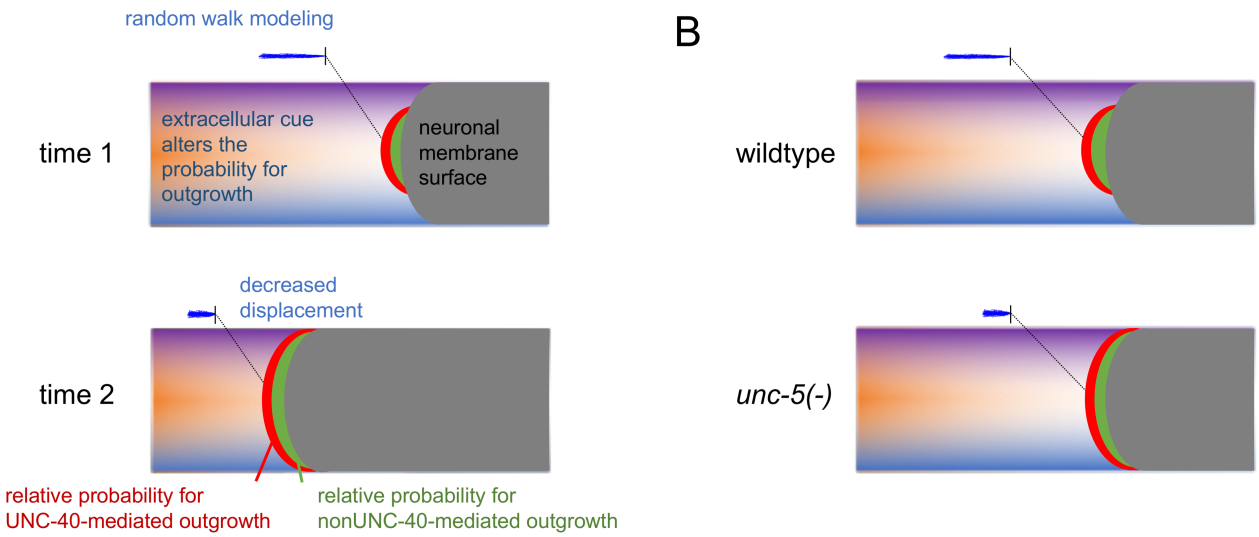
A
random walk modeling
time 1
extracellular cue alters the probability for outgrowth
neuronal membrane surface
decreased displacement
time 2
relative probability for UNC-40-mediated outgrowth
relative probability for nonUNC-40-mediated outgrowth
B
wildtype
unc-5(-)

1164

1165 **Figure 3. UNC-5 regulates the patterning of outgrowth extensions from HSN.** (**A**)
1166 Photomicrographs of HSN at the L1, L2, and adult stages in wildtype and *unc-5(e53)* mutants.
1167 In L1 and L2 animals neurite extensions (arrows) are often observed in wild-type animals but
1168 are more rare in *unc-5* mutants. The short ventral migration of the cell body that occurs in
1169 wild-type animal sometimes fails in *unc-5* mutants, leaving the cell body farther from the PLM
1170 axon (arrowhead) with a single longer ventral extension. The position of the cell body remains
1171 dorsal. Scale bar: 10 μm. (**B**) The percentage of HSN neuron with 0, 1, or more than 1 neurite
1172 extension at the L1 stage. In *unc-5* mutants nearly half of the neurons do not extend a process.
1173 Error bars indicated the standard error mean; n values are indicated above each column.
1174 Significant differences (two-tailed t-test), *P<0.001. (**C**) The percentage of HSN neurons with a
1175 single long extension at the L2 stage. Several *unc-5* alleles were tested as described in the text.
1176 In mutants with loss-of-function there is more often a single extension from the cell body and
1177 the cell body is dorsally mispositioned. (**D**) Photomicrographs of HSN at the early L4, late L4,
1178 and adult stages in wildtype and in animals expressing UNC-6ΔC. The expression of UNC-6ΔC
1179 induces multiple processes, most often two major extensions, that are guided ventrally. (**E**) The
1180 percentage of HSN neurons with a cell body mispositioned dorsally at the L2 stage. In loss-of-
1181 function mutants the cell body often fails to undertake a short ventral migration during the L2
1182 stage. The migration is not delayed, but rather it remains dorsal. (**F**) The percentage of HSN
1183 neurons with multiple ventral extensions at the L4 stage. The additional processes induced by
1184 UNC-6ΔC can be suppressed by *unc-5* and *mig-10* mutations. Additional processes induced by
1185 *mig-15(rh148)* can also be suppressed by the *unc-5* mutation. (**G**) Photomicrographs of HSN at
1186 adult stages in a *mig-15* mutant. Similar to UNC-6ΔC expression, *mig-15* mutations can also
1187 cause additional processes that are guided ventrally (YANG *et al.* 2014).

1188

1189

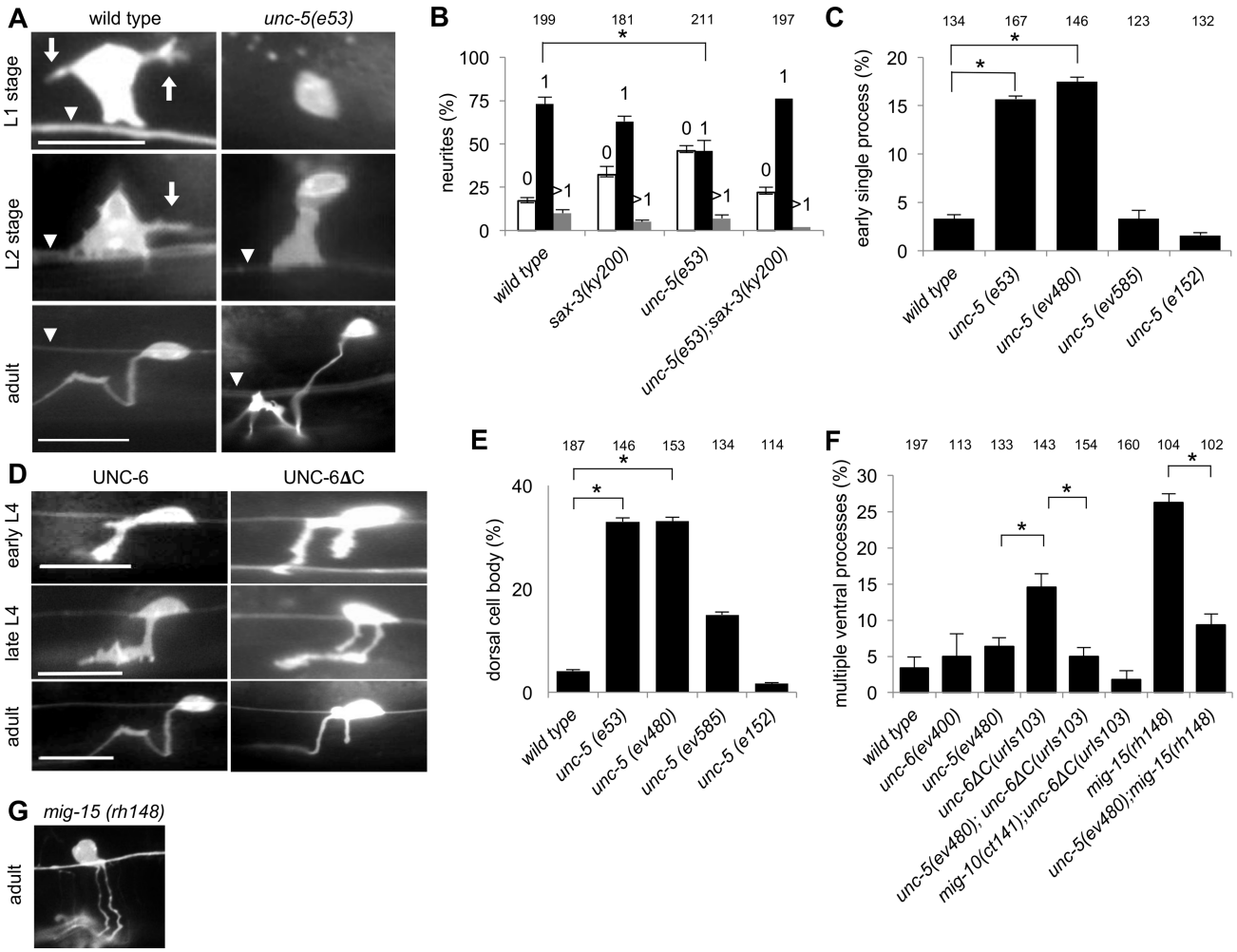
A
wild type
unc-5(e53)
L1 stage
L2 stage
adult
B
199
181
211
197
neurites (%)
wild type
sax-3(ky200)
unc-5(e53)
unc-5(e53);sax-3(ky200)
C
134
167
146
123
132
early single process (%)
wild type
unc-5 (e53)
unc-5 (ev480)
unc-5 (ev585)
unc-5 (e152)
D
UNC-6
UNC-6ΔC
early L4
late L4
adult
E
187
146
153
134
114
dorsal cell body (%)
wild type
unc-5 (e53)
unc-5 (ev480)
unc-5 (ev585)
unc-5 (e152)
F
197
113
133
143
154
160
104
102
multiple ventral processes (%)
wild type
unc-6(ev400)
unc-5(ev480)
unc-6ΔC(urls103)
unc-5(ev480); unc-6ΔC(urls103)
mig-10(ct141);unc-6ΔC(urls103)
mig-15(rh148)
unc-5(ev480);mig-15(rh148)
G
mig-15 (rh148)
adult

1190

1191 **Figure 4 UNC-5 regulates the patterning of extension from ALM, AVM, and PLM.** (**A**)
1192 Photomicrographs of the ALM, AVM, and PLM neurons at the L4 stage in wild-type animals and
1193 *mig-15* mutants. In wildtype (top) a single PLM axon travels anteriorly from the posterior cell
1194 body (not shown). Near the vulva (arrow) the axon branches; one branch extends to the
1195 ventral nerve chord and another extends anteriorly. The anterior extension terminates before
1196 reaching the area of the ALM cell body. In *mig-15* mutants the PLM can extend anteriorly past
1197 the ALM cell body (bottom). (**B**) The percentage of PLM neurons where the PLM neuron
1198 extend anteriorly past the ALM cell body. The anterior extension often over-extends in *mig-15*
1199 mutants. Loss of *unc-5* or *unc-40* function can suppress this phenotype. (**C**) Photomicrographs
1200 of the ALM and AVM neurons at the L4 stage in wild-type animals and mutants showing
1201 different patterns of outgrowth extension. In wildtype (top) a single axon travels anteriorly to
1202 the nerve ring (arrowheads). At the nerve ring the axon branches; one branch extends further
1203 anteriorly and the other extends into the nerve ring. In mutants, one or both axons may only
1204 extend anteriorly and will not extend into the nerve ring (second from top). Or one or both
1205 axons will only extend into the nerve ring and will not extend anteriorly (third from top). Or
1206 one or both axons will fail to extend into either the nerve ring or anteriorly (bottom). Scale bar:
1207 20 μm. (**D**) The percentage of AVM neurons where the AVM neuron failed to extend into the
1208 nerve ring. The neuron often fails to extend in the *unc-40* and *mig-15;unc-5* mutants, whereas it
1209 does extend in the *mig-15, unc-5,* and *mig-15;unc-40* mutants. Error bars indicated the standard
1210 error mean; n values are indicated above each column. Significant differences (two-tailed t-
1211 test), *P<0.001. (**E**) The percentage of AVM neurons where the AVM neuron failed to extend
1212 anteriorly, past the nerve ring. The neuron often fails to extend anteriorly in the *mig-15;unc-5*
1213 mutants, whereas it does extend in the *mig-15, unc-5, unc-40,* and *unc-40;mig-15* mutants. There
1214 is a significant difference between the *unc-40* and *unc-40;mig-15* mutants.

1215
1216

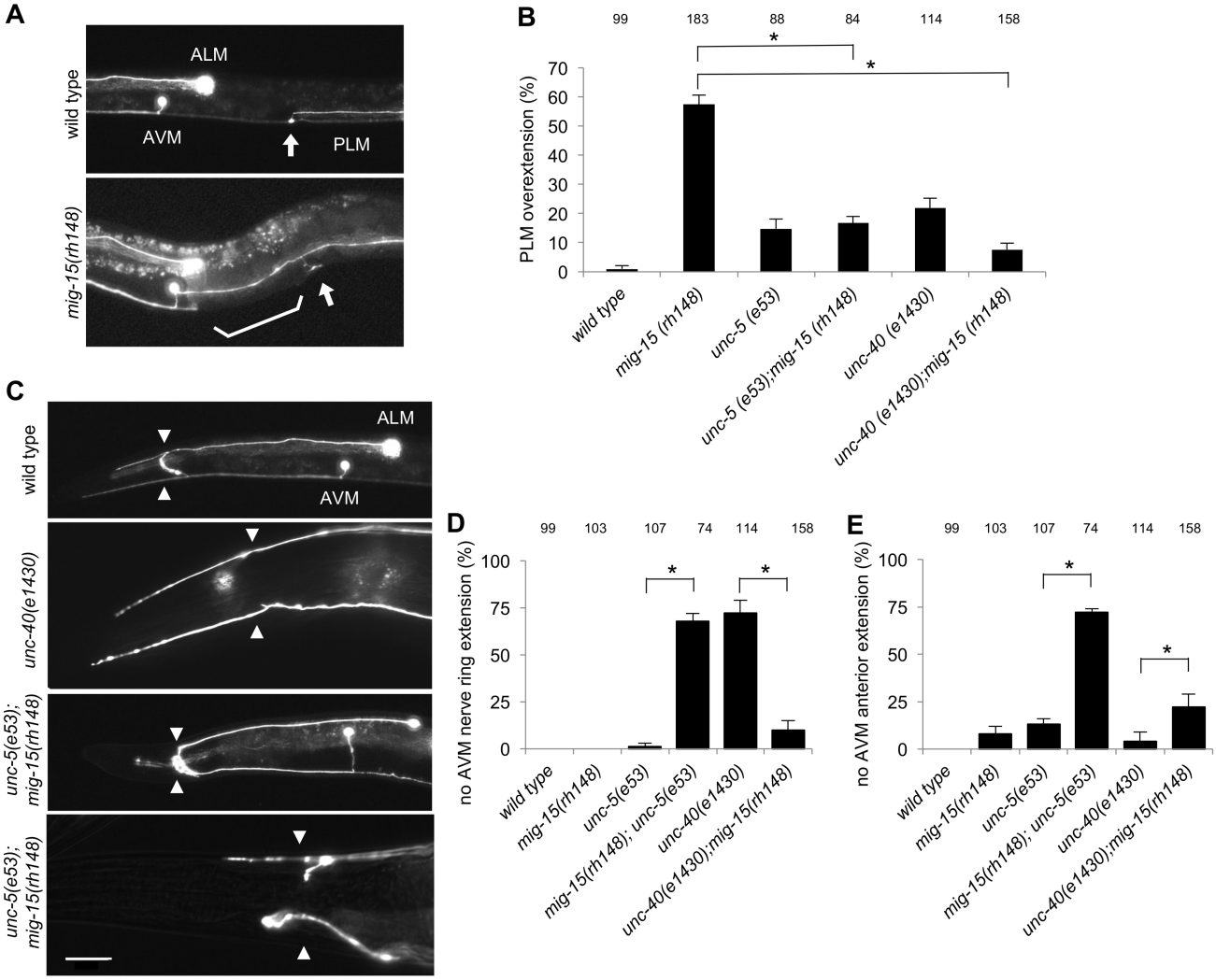
A
wild type
ALM
AVM
PLM
mig-15(rh148)
B
99
183
88
84
114
158
PLM overextension (%)
70
60
50
40
30
20
10
0
wild type
mig-15 (rh148)
unc-5 (e53)
unc-5 (e53);mig-15 (rh148)
unc-40 (e1430)
unc-40 (e1430);mig-15 (rh148)
C
wild type
ALM
AVM
unc-40(e1430)
unc-5(e53); mig-15(rh148)
unc-5(e53); mig-15(rh148)
D
99
103
107
74
114
158
no AVM nerve ring extension (%)
100
75
50
25
0
wild type
mig-15(rh148)
unc-5(e53)
mig-15(rh148); unc-5(e53)
unc-40(e1430)
unc-40(e1430);mig-15(rh148)
E
99
103
107
74
114
158
no AVM anterior extension (%)
100
75
50
25
0
wild type
mig-15(rh148)
unc-5(e53)
mig-15(rh148); unc-5(e53)
unc-40(e1430)
unc-40(e1430);mig-15(rh148)

1217
1218

1219 **Figure 5 Assay to measure the effects a mutation has on movement.** (**A**) The direction of
1220 outgrowth extension from the HSN cell body can vary and whether the axon developed in the
1221 dorsal, anterior, posterior, or ventral direction in L4 stage animals is scored (left panel). This
1222 creates a probability distribution in which the direction (*X*) is a random variable (center panel).
1223 A simple random walk is generated by using the same probability distribution for a succession
1224 of steps with an equal time interval (right panel). (**B**) For wildtype and two mutants, 50
1225 simulated random walks of 500 steps were plotted from an origin (0,0). The results graphically
1226 indicate the directional bias for movement. For random walk movement created in mutant A
1227 (red, results from *unc-5(e53)*), the directional bias is shifted anteriorly (left) relative to
1228 wildtype. The results also graphically show the displacement of movement. For random walk
1229 movement created in mutant B (blue, results from *egl-20(n585);sax-3(ky123)*), the average of
1230 the final position (displacement) from the origin is a much shorter distance than wildtype. (**C**)
1231 Plots of the normal distribution of the final position along the x axis of the random walk tracks
1232 shown in B. The mean position for each is set at 0. The plots graphically illustrate how random
1233 walks constructed from the probability distribution for the direction of outgrowth extensions
1234 can reveal a diffusion process.
1235

1236

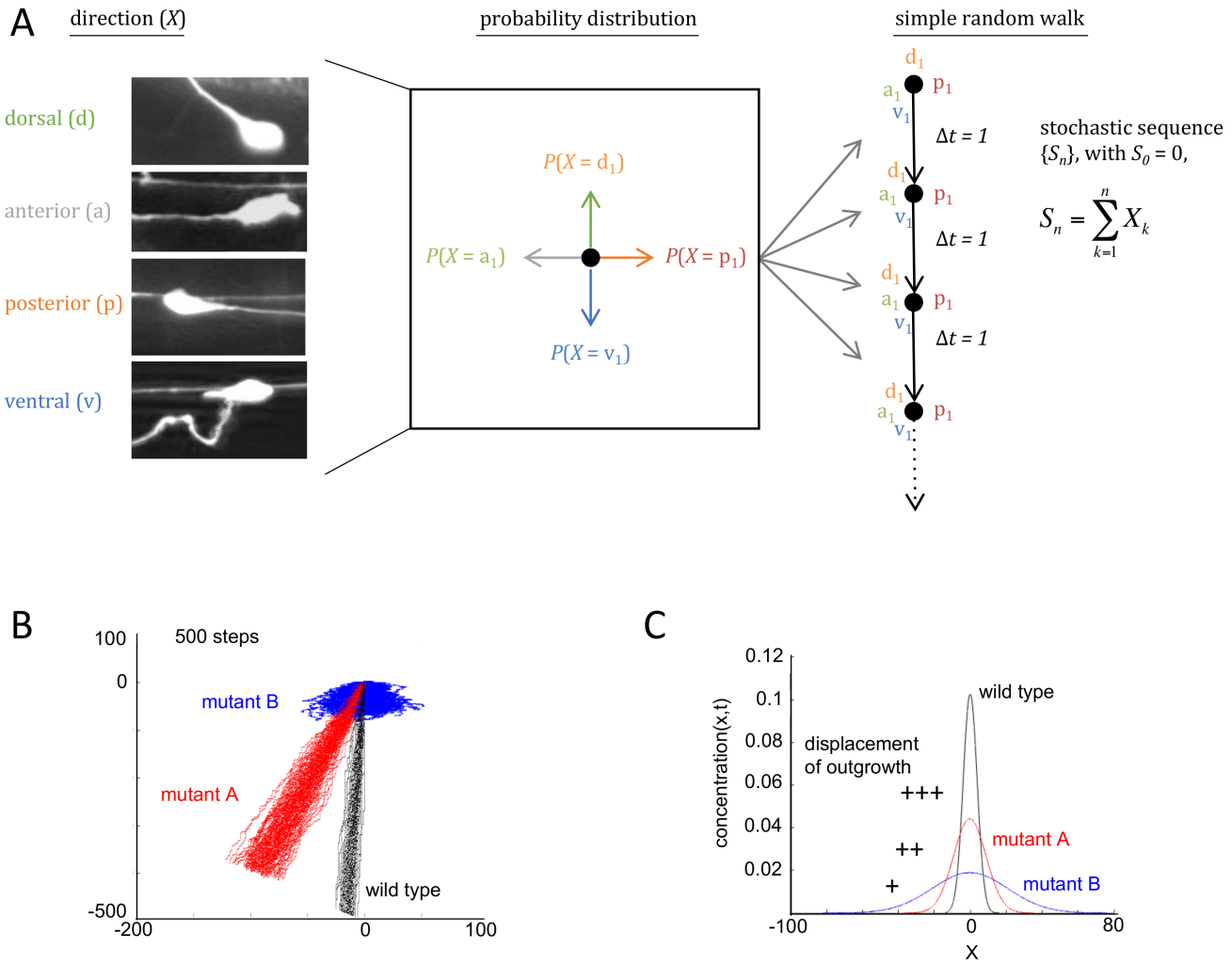
A
direction (X)
probability distribution
simple random walk
dorsal (d)
anterior (a)
posterior (p)
ventral (v)
P(X = d1)
P(X = a1)
P(X = p1)
P(X = v1)
Δt = 1
stochastic sequence
{Sn}, with S0 = 0,
Sn = Σ Xk
B
500 steps
mutant B
mutant A
wild type
100
0
-500
-200
0
100
C
wild type
displacement
of outgrowth
+++
++
+
mutant A
mutant B
concentration(x,t)
0.12
0.1
0.08
0.06
0.04
0.02
-100
0
80
X

1237

1238 **Figure 6. Mutations have different effects on movement.** Examples of random walk
1239 analyses using the direction of axon development from the HSN neuron in different mutants
1240 (Table 1). The graphs were created as described in the figure legend of Figure 3. For each
1241 panel, plots are shown for the normal distribution of the final position along the x axis for the
1242 random walk tracks plotted in the inserts. The inserts depict the random walk movement that
1243 would be produced by the probability distribution for the direction of outgrowth in the mutant.
1244 Plots derived from the same data are colored alike. Each panel depicts the analyses of four
1245 different mutants and wildtype. Three different distribution patterns are observed: (1) the
1246 wild-type distribution, which has the distribution curve with the highest peak; (2) the *unc-5,*
1247 *egl-20, unc-53,* and *unc-6* (not shown) distribution, which is flatter than the wild-type curve; (3)
1248 the *madd-2, sax-3, mig-15,* and double combinations, which have the flattest distribution curve.
1249

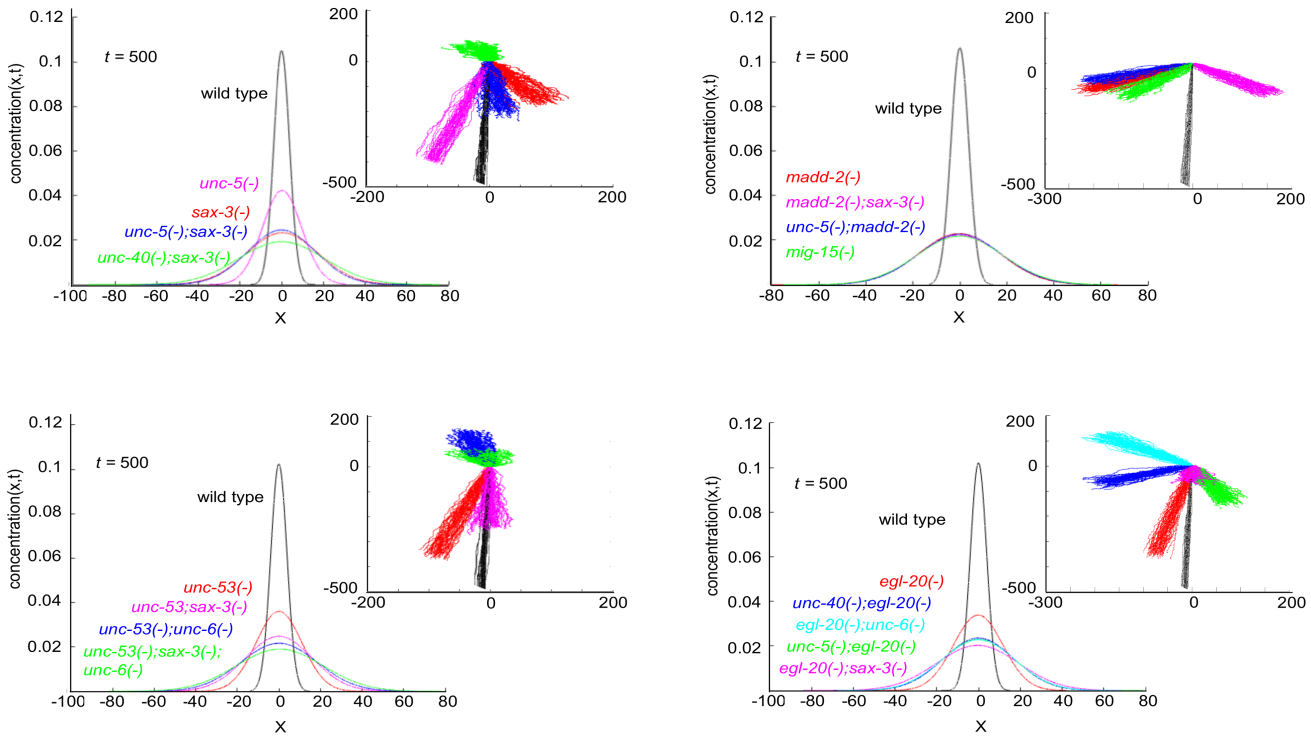
t = 500
wild type
unc-5(-)
sax-3(-)
unc-5(-);sax-3(-)
unc-40(-);sax-3(-)
concentration(x,t)
X
madd-2(-)
madd-2(-);sax-3(-)
unc-5(-);madd-2(-)
mig-15(-)
unc-53(-)
unc-53;sax-3(-)
unc-53(-);unc-6(-)
unc-53(-);sax-3(-);
unc-6(-)
egl-20(-)
unc-40(-);egl-20(-)
egl-20(-);unc-6(-)
unc-5(-);egl-20(-)
egl-20(-);sax-3(-)

1252 **Figure 7. Mutations alter the spatial extent of movement.** (**A**) Plotted are the mean
1253 squared displacement (MSD) curves as a function of time interval (d*t*). The values are in
1254 arbitrary units, since the time scale was arbitrarily set at 1. The curves show the extent that
1255 different mutations can alter the MSD relative to wildtype and the MSD caused by an unbiased
1256 random walk. For each time interval, mean and s.e.m. are plotted. (**B**) From the slope of MSD
1257 curves a coefficient can be derived that gives the relative rate of diffusion. Colored bars
1258 correspond to the like-colored curves given in panel A. The coefficients for *unc-5, egl-20, unc-*
1259 *53,* and *unc-6* form a class that is distinct from that derived from wildtype and from the double
1260 mutants.

1261
1262

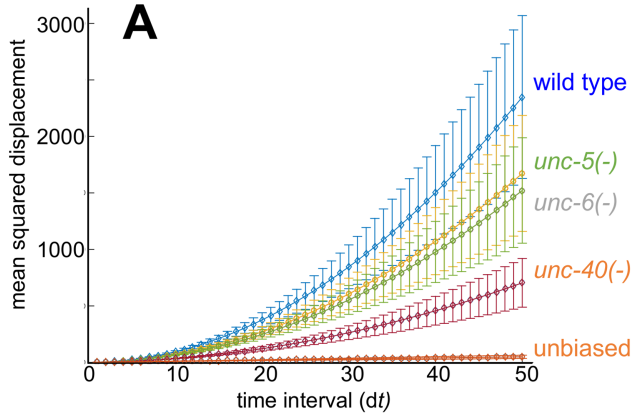
A
mean squared displacement
3000
2000
1000
0
10
20
30
40
50
time interval (dt)
wild type
unc-5(-)
unc-6(-)
unc-40(-)
unbiased

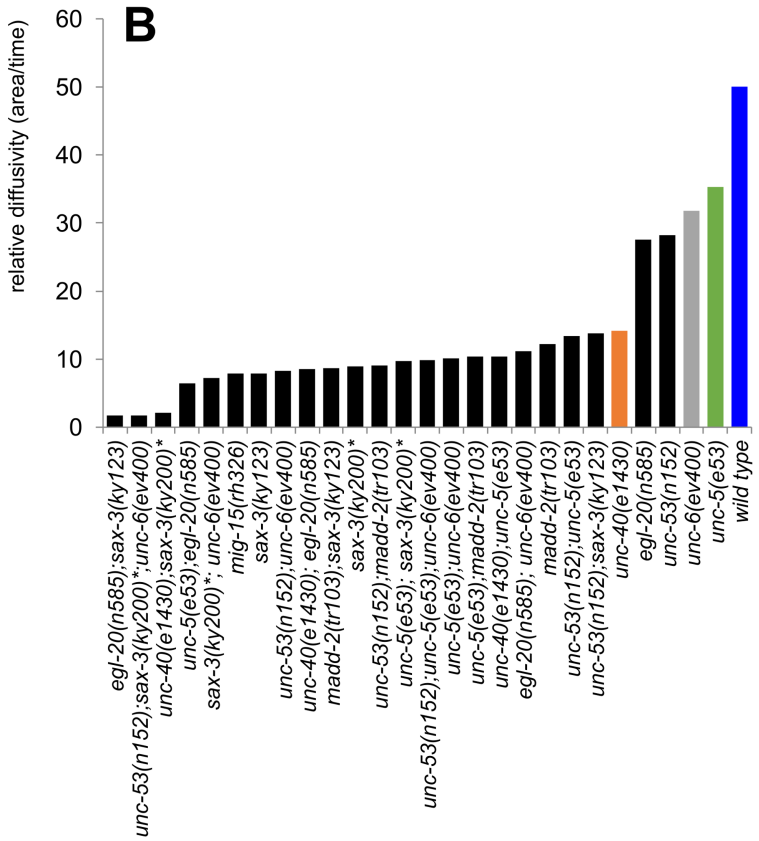
B
relative diffusivity (area/time)
60
50
40
30
20
10
0
egl-20(n585);sax-3(ky123)
unc-53(n152);sax-3(ky200)*;unc-6(ev400)
unc-40(e1430);sax-3(ky200)*
unc-5(e53);egl-20(n585)
sax-3(ky200)*; unc-6(ev400)
mig-15(rh326)
sax-3(ky123)
unc-53(n152);unc-6(ev400)
unc-40(e1430); egl-20(n585)
madd-2(tr103);sax-3(ky123)
sax-3(ky200)*
unc-53(n152);madd-2(tr103)
unc-5(e53); sax-3(ky200)*
unc-53(n152);unc-5(e53);unc-6(ev400)
unc-5(e53);unc-6(ev400)
unc-5(e53);madd-2(tr103)
unc-40(e1430);unc-5(e53)
egl-20(n585); unc-6(ev400)
madd-2(tr103)
unc-53(n152);unc-5(e53)
unc-53(n152);sax-3(ky123)
unc-40(e1430)
egl-20(n585)
unc-53(n152)
unc-6(ev400)
unc-5(e53)
wild type

1265 **Figure 8. Models for the relationship between UNC-40-mediated outgrowth activity and**
1266 **UNC-40 receptor clustering. (A)** In this model the self-organizing UNC-40 SOAL process
1267 causes observable UNC-40 receptor clustering. Receptor clusters become stable and exit the
1268 SOAL process, at which point they recruit the outgrowth machinery. Whereas the direction of
1269 asymmetric receptor localization is determined stochastically, the direction of outgrowth is
1270 determined by the site of stabilization. **(B)** In this model the self-organizing UNC-40 SOAL
1271 process is coupled to the outgrowth machinery. The direction of both asymmetric receptor
1272 localization and outgrowth activity are stochastically determined. Observable receptor
1273 clustering may arise over time and these sites may become paramount for outgrowth
1274 movement, but cluster formation is not a prerequisite for outgrowth activity. Conceptually, in
1275 both models the site of outgrowth activity is determined by where UNC-40 receptor complexes
1276 recruit the outgrowth machinery, however the second model postulates situations where there
1277 are innumerable fluctuating sites that create outgrowth movement in various directions.
1278 Because the effect at each instance of time of every outgrowth event is immeasurable,
1279 outgrowth in this model is considered as a continuous stochastic process that evolves over
1280 time.
1281
1282
1283
1284
1285

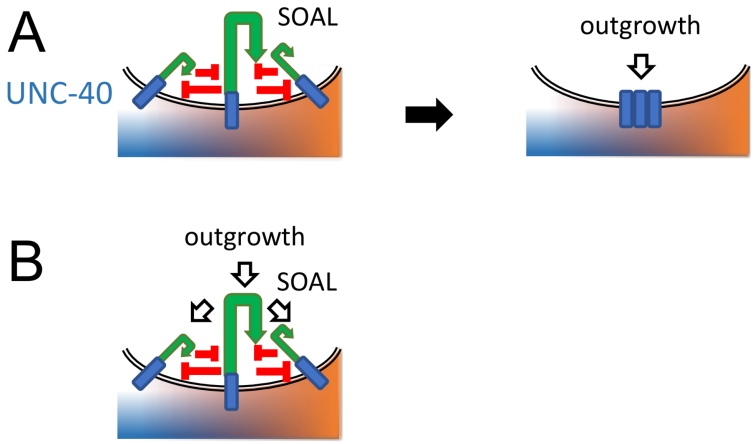

1286

1287

1288 **Figure 9. Mutations affect asymmetric intracellular UNC-40::GFP localization.** (**A**) Graph
1289 indicating the dorsal-ventral localization of UNC-40::GFP in HSN. The graph shows the average
1290 ratio of dorsal-to-ventral intensity from linescan intensity plots of the UNC-40::GFP signal
1291 around the periphery of the HSN cell. UNC-40::GFP is ventrally localized in wildtype, but the
1292 ratio is different in the mutants. Error bars represent standard error of mean. Below is a
1293 graphic representation of the possible UNC-40 localization patterns when the intensity ratio is
1294 ≥ 1 or is <1. (**B**) Graph indicating the anterior-posterior localization of UNC-40::GFP. To
1295 determine orientation, line-scan intensity plots of the UNC-40::GFP signal across the dorsal
1296 periphery of the HSN cell were taken, the dorsal surface was geometrically divided into three
1297 equal segments, and the total intensity of each was recorded. The percent intensity was
1298 calculated for each segment and ANOVA was used to determine if there is a significant
1299 difference between the three segments (see Material and Methods). Whereas in the *unc-5* and
1300 *egl-20* mutants there is a bias for anterior or posterior localization, there is a uniform
1301 distribution in *unc-5;egl-20* double mutants. Uniform distribution is also observed in strong
1302 loss-of-function *sax-3* and *madd-2* mutants. (*) Animals grown at the *sax-3(ky200)* restrictive
1303 temperature (25°C). Below is a graphic representation of the possible UNC-40 localization
1304 patterns.
1305

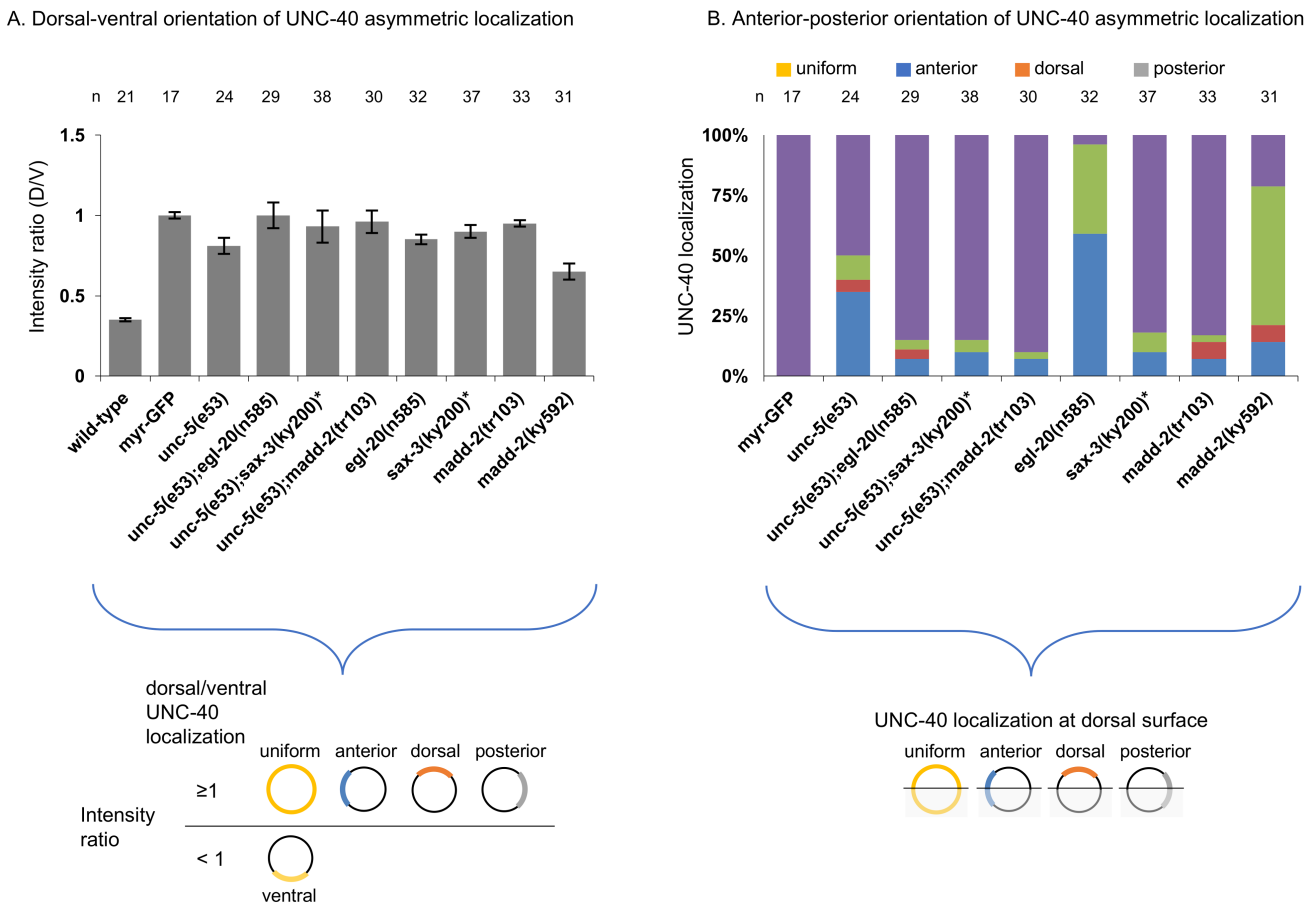
A. Dorsal-ventral orientation of UNC-40 asymmetric localization
n 21 17 24 29 38 30 32 37 33 31
Intensity ratio (D/V)
1.5
1
0.5
0
wild-type
myr-GFP
unc-5(e53)
unc-5(e53);egl-20(n585)
unc-5(e53);sax-3(ky200)*
unc-5(e53);madd-2(tr103)
egl-20(n585)
sax-3(ky200)*
madd-2(tr103)
madd-2(ky592)
dorsal/ventral UNC-40 localization
uniform
anterior
dorsal
posterior
Intensity ratio
≥1
< 1
ventral
B. Anterior-posterior orientation of UNC-40 asymmetric localization
uniform
anterior
dorsal
posterior
n 17 24 29 38 30 32 37 33 31
UNC-40 localization
100%
75%
50%
25%
0%
myr-GFP
unc-5(e53)
unc-5(e53);egl-20(n585)
unc-5(e53);sax-3(ky200)*
unc-5(e53);madd-2(tr103)
egl-20(n585)
sax-3(ky200)*
madd-2(tr103)
madd-2(ky592)
UNC-40 localization at dorsal surface
uniform
anterior
dorsal
posterior

1306

1307

1308 **Figure 10. Model for the outgrowth movement of PLM.** Schematic diagrams of the
1309 anteriorly directed outgrowth of PLM. The elements of the schematics are described in Figure
1310 2. **(A)** At each of the four positions an extension encounters different levels of extracellular
1311 cues. At position 3, a cue(s) is present that inhibits outgrowth activity. PLM extension
1312 terminates in this area in wildtype, but in some mutants there is an overextension to position 4.
1313 **(B)** Depicted are the effects that extracellular cues have on the relative probabilities of UNC-40-
1314 mediated and nonUNC-40-mediated outgrowth activity at the different positions. At position 3
1315 in wildtype the degree to which the direction of outgrowth activity fluctuates increases and the
1316 extent of outgrowth movement decreases, stalling outgrowth. Because the SOAL process is
1317 perturbed in the mutants, at position 3 the probability of outgrowth activity perpendicular to
1318 the direction bias does not increase as much as in wildtype and the probability of anterior
1319 outgrowth activity remains greater. This allows a stronger directional bias to persist, allowing
1320 forward extension. To illustrate the concept, random walk models are shown which were
1321 constructed using the indicated values for outgrowth in the anterior, dorsal, and ventral
1322 directions. See text for details.
1323
1324

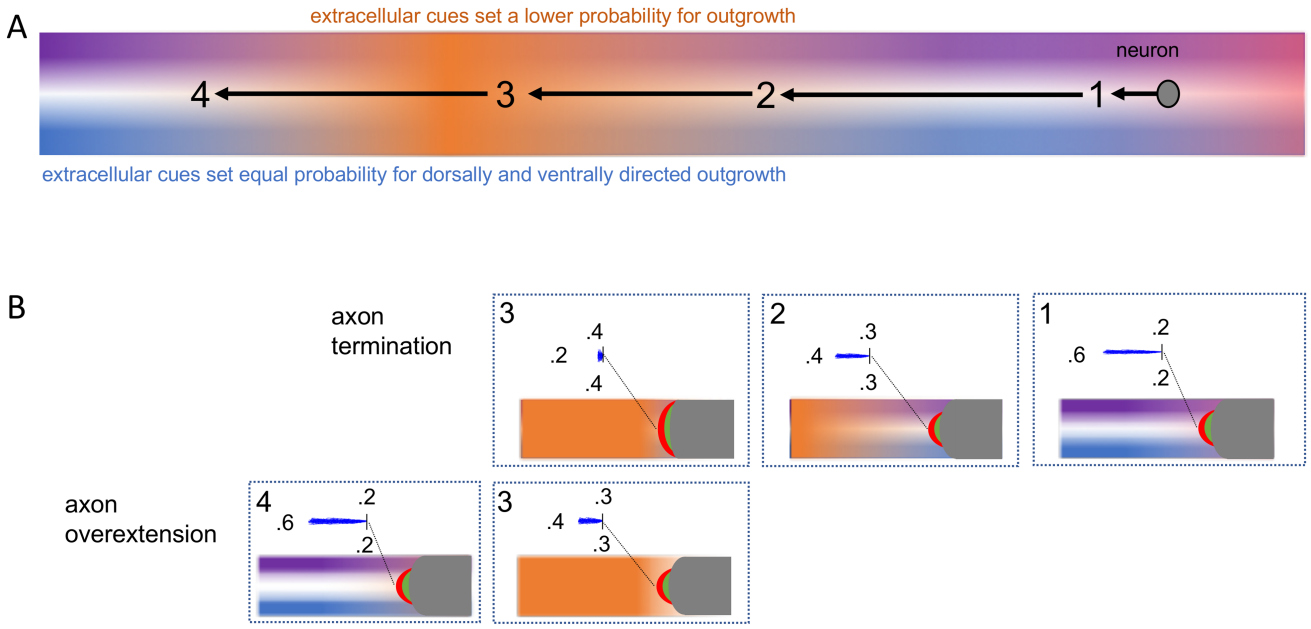
A
extracellular cues set a lower probability for outgrowth
neuron
4
3
2
1
extracellular cues set equal probability for dorsally and ventrally directed outgrowth
B
axon termination
3
.4
.2
.4
2
.3
.4
.3
1
.2
.6
.2
axon overextension
4
.2
.6
.2
3
.3
.4
.3

1325

1326

1327 **Figure 11. Model for the effects that mutations have on the outgrowth movement of PLM.**
1328 Schematic diagrams of PLM outgrowth at position 3 of Figure 10 in wildtype and mutants. The
1329 elements of the schematics are described in Figure 2. PLM outgrowth terminates in wildtype,
1330 *unc-40*, and *unc-5;mig-15* mutants, but overextends in *mig-15* mutants. See text for details.
1331
1332

figure 10, position 3

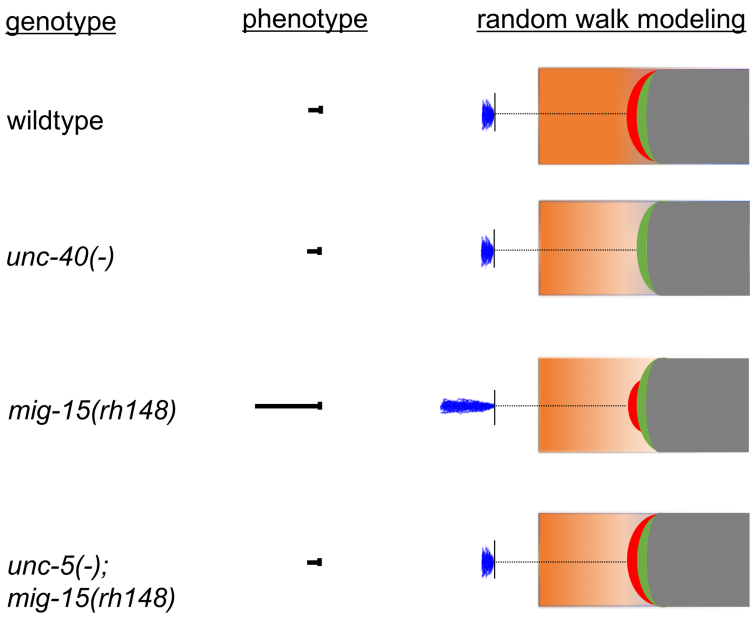

1335 **Figure 12. Model for the outgrowth movement of AVM at the nerve ring.** Schematic
1336 diagrams of the outgrowth of AVM at the nerve ring. The elements of the schematics are
1337 described in Figure 2. **(A)** At each of the four positions an extension encounters different
1338 levels of extracellular cues. At position 2, a cue(s) at the nerve ring promotes UNC-40-mediated
1339 outgrowth activity. From this position in wildtype, AVM extends further anteriorly and also
1340 dorsally along the nerve ring. However, in some mutants either the anterior or dorsal
1341 extension is absent. In other mutants, extension in both directions is absent. **(B)** Depicted are
1342 the effects that extracellular cues have on the relative probabilities of UNC-40-mediated and
1343 nonUNC-40-mediated outgrowth activity at the different positions. At position 2 in wildtype
1344 the extracellular cues create a weak bias for outgrowth in both the anterior and dorsal
1345 directions. Further dorsally at position 3, cues create an equal probability for outgrowth in the
1346 anterior and posterior directions, allowing the nerve ring cue that promotes UNC-40-mediated
1347 outgrowth to maintain a dorsal directional bias. Further anteriorly at position 4, cues create an
1348 equal probability for outgrowth in the dorsal and ventral directions, allowing anterior cues that
1349 promote outgrowth to create an anterior directional bias. To illustrate the concept, random
1350 walk models are shown which were constructed using the indicated values for outgrowth in the
1351 indicated directions. See text for details.
1352
1353
1354
1355
1356

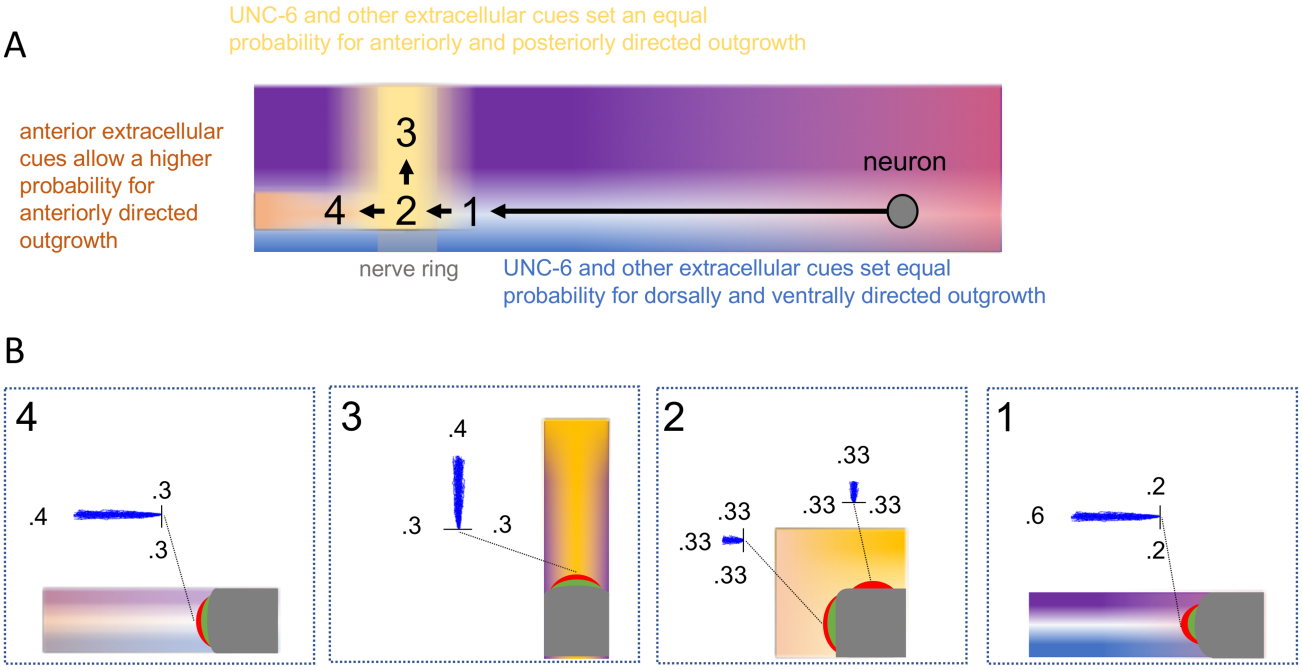
A
UNC-6 and other extracellular cues set an equal probability for anteriorly and posteriorly directed outgrowth
anterior extracellular cues allow a higher probability for anteriorly directed outgrowth
3
4
2
1
neuron
nerve ring
UNC-6 and other extracellular cues set equal probability for dorsally and ventrally directed outgrowth
B
4
.4
.3
.3
3
.4
.3
.3
2
.33
.33
.33
.33
.33
1
.6
.2
.2

1359 **Figure 13. Model for the effects that mutations have on the outgrowth movement of AVM**
1360 **at the nerve ring.** Schematic diagrams of AVM outgrowth at position 2 of Figure 12 in
1361 wildtype and mutants. The elements of the schematics are described in Figure 2. AVM
1362 outgrowth extends both anteriorly and dorsally from this position in wildtype, *mig-15,* and *unc-*
1363 *40;mig-15* mutants. Dorsal extensions are often absent in *unc-40* mutants, whereas both
1364 anterior and dorsal extensions are absent in *unc-5;mig-15* mutants. See text for details.
1365
1366
1367
1368
1369

figure 12, position 2

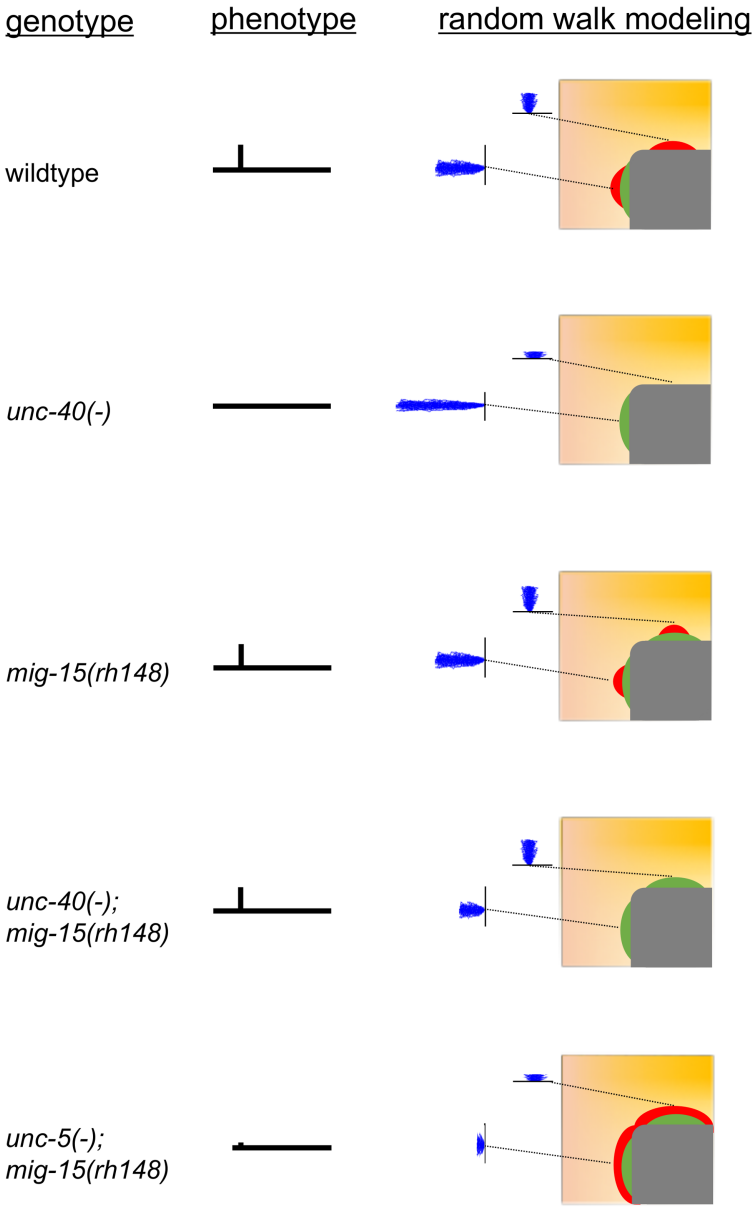

1373 **Figure 14. Model for the outgrowth movement of HSN.** Schematic diagrams of the ventrally
1374 directed outgrowth of HSN. The elements of the schematics are described in Figure 2. **(A)** At
1375 each of the three positions an extension encounters different levels of extracellular cues. At
1376 position 3, a cue(s) is present that promotes outgrowth activity. At the time when extension is
1377 first observed in wildtype, extension is absent in some mutants. Nevertheless, ventral
1378 extension will be complete in the mutants at about the same time as in wildtype. **(B)** Depicted
1379 are the effects that extracellular cues have on the relative probabilities of UNC-40-mediated and
1380 nonUNC-40-mediated outgrowth activity at the different positions. Compared to wildtype, at
1381 position 1 in mutants with delayed protrusion the degree to which the direction of outgrowth
1382 activity fluctuates is greater and the extent of outgrowth movement is less, resulting in a
1383 reduced rate of outgrowth. A weak ventral directional bias develops in the mutant that allows
1384 initial ventral extension and by position 2 this ventral bias is stronger. At position 3 in both
1385 wildtype and mutant, the degree to which the direction of outgrowth activity fluctuates
1386 increases and the extent of outgrowth movement decreases. To illustrate the concept, random
1387 walk models are shown which were constructed using the indicated values for outgrowth in the
1388 anterior, posterior, and ventral directions. See text for details.
1389
1390
1391

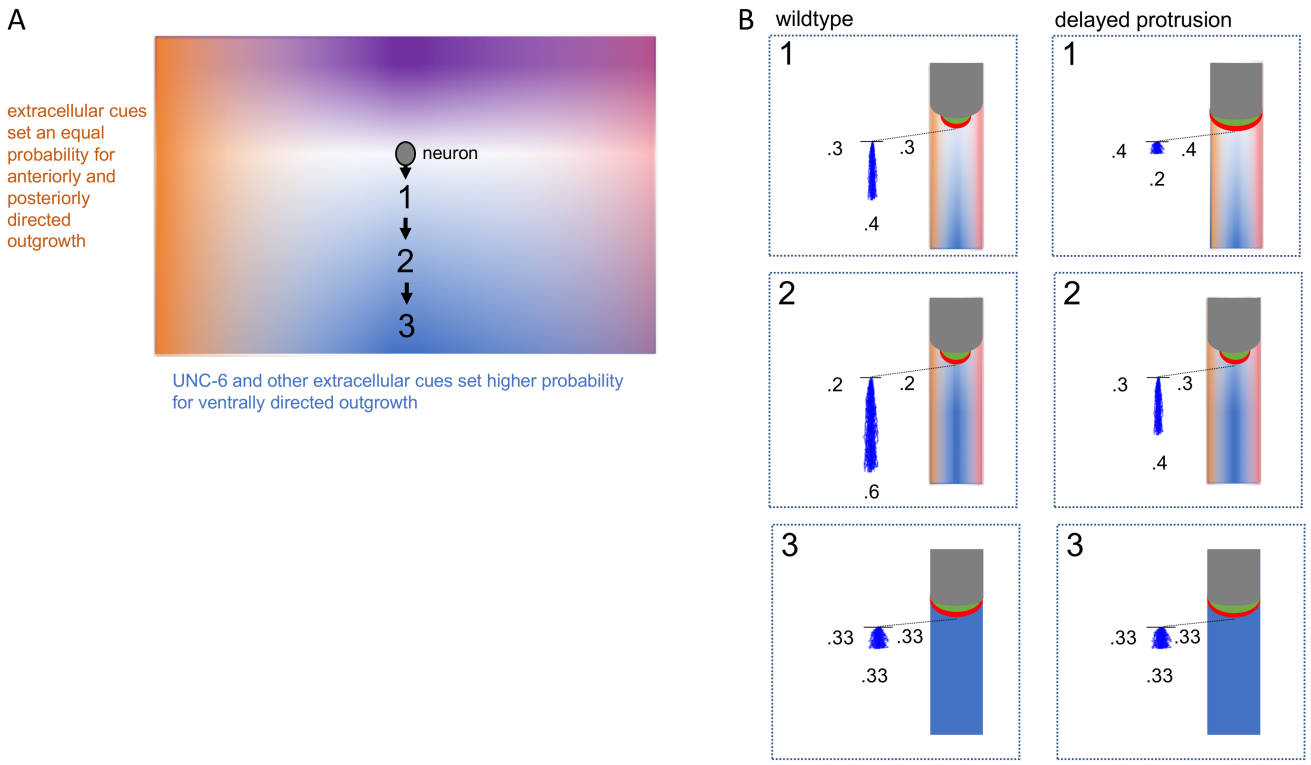
A
extracellular cues set an equal probability for anteriorly and posteriorly directed outgrowth
neuron
1
2
3
UNC-6 and other extracellular cues set higher probability for ventrally directed outgrowth
B
wildtype
delayed protrusion
1
.3
.3
.4
1
.4
.4
.2
2
.2
.2
.6
2
.3
.3
.4
3
.33
.33
.33
3
.33
.33
.33

1392

1393 **Figure 15. Model for the effects that mutations have on the outgrowth movement of HSN.**
1394 **(A)** Schematic diagrams of HSN outgrowth at position 1 of Figure 14 in wildtype and mutants.
1395 The elements of the schematics are described in Figure 2. HSN outgrowth is delayed in *unc-5*
1396 mutants and can develop multiple processes in *mig-15* mutants. The multiple process
1397 phenotype is suppressed in *unc-5;mig-15* mutants. See text for details. **(B)** Schematic diagrams
1398 of the development of multiple process that maintain the same directional bias. The process is
1399 shown in three steps. At the first step, UNC-40 receptors (blue rectangles) are trafficked to the
1400 membrane as part of the UNC-40 SOAL process (blue arrows). At the second step, UNC-5
1401 signaling alters the trafficking, increasing the rates anterior (orange arrows) and posterior (red
1402 arrows). By the third step, the rate of outgrowth at the flanking regions is greater. We propose
1403 that UNC-40, UNC-5, and UNC-6 can be considered as components of an activator-inhibitor
1404 system which allows outgrowth patterns to self-organize. See text for details.
1405
1406
1407
1408
1409

1410

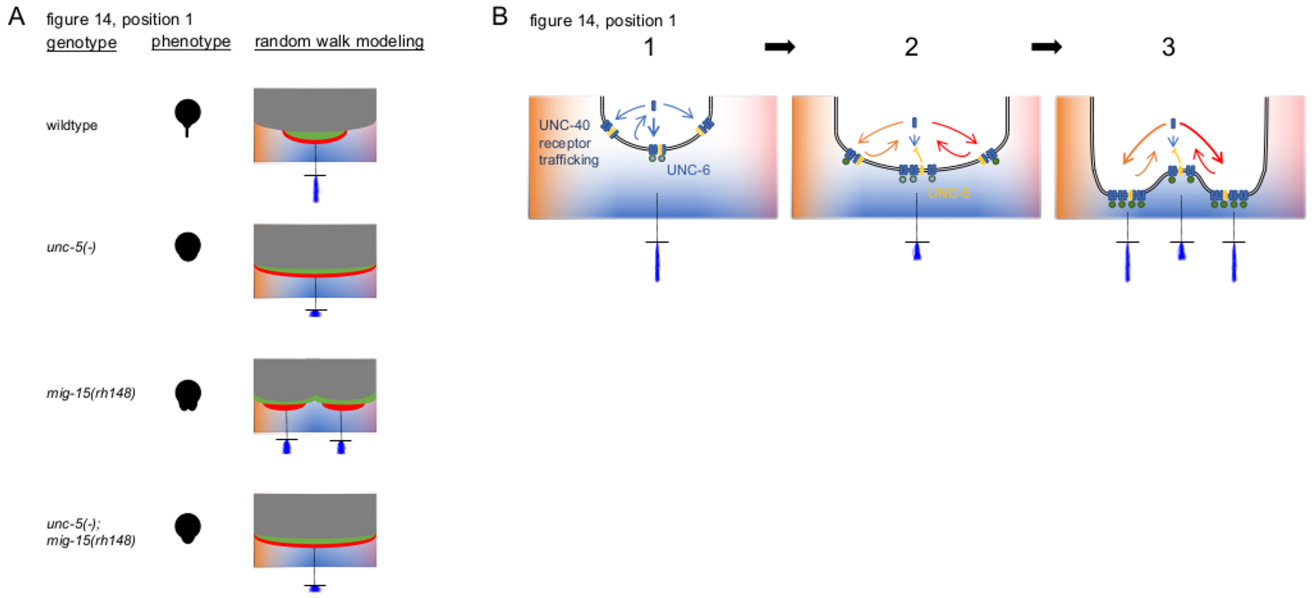

1411

1412

1413 **Figure 16. Genetic pathways for self-organizing UNC-40 asymmetric localization.** (**A**)
1414 Table summarizing the results of experiments previously reported and described in Figure 9 of
1415 this paper. (**B**) The genetic data support a model whereby the UNC-6 and EGL-20 extracellular
1416 cues regulate at least three pathways leading to robust asymmetric UNC-40 localization.
1417 Robust asymmetric UNC-40 localization refers to the ability to observe UNC-40::GFP clustering
1418 at the surface of the neuron. Arrows represent activation; bars represent repression. See text
1419 for the logic used to construct the pathways.
1420

A

loss-of-function			robust asymmetric UNC-40 localization	reference
unc-6			no	(Kulkarni et al., 2013)
unc-5			yes	(Kulkarni et al., 2013)
unc-5	*unc-6*		no	(Kulkarni et al., 2013)
unc-5	*egl-20*		no	
unc-5	*sax-3*		no	
unc-5	*unc-53*		no	(Kulkarni et al., 2013)
unc-5	*unc-53*	*unc-6*	yes	(Kulkarni et al., 2013)
unc-5	*unc-53*	*sax-3*	no	
unc-5	*madd-2*		no	
unc-6	*unc-53*		yes	(Kulkarni et al., 2013)
unc-6	*sax-3*		no	(Tang and Wadsworth, 2014)
unc-6	*unc-53*	*sax-3*	no	(Tang and Wadsworth, 2014)
egl-20			yes	(Kulkarni et al., 2013)
egl-20	*unc-53*		yes	(Kulkarni et al., 2013)
egl-20	*unc-6*		no	(Kulkarni et al., 2013)
egl-20	*sax-3*		no	(Tang and Wadsworth, 2014)
sax-3			no	(Tang and Wadsworth, 2014)
sax-3	*unc-53*		no	(Tang and Wadsworth, 2014)
unc-53			yes	(Kulkarni et al., 2013)
madd-2			no	
mig-15			yes	(Yang et al., 2014)

B

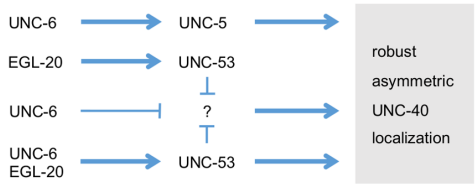

1421